ISSN 2096-7071 (Print)
ISSN 2097-3101 (Online)
CN 10-1629/R1

CHINA CDC WEEKLY

Vol. 8 No. 3 Jan. 16, 2026

CCDC weekly

中国疾病预防控制中心周报(英文)

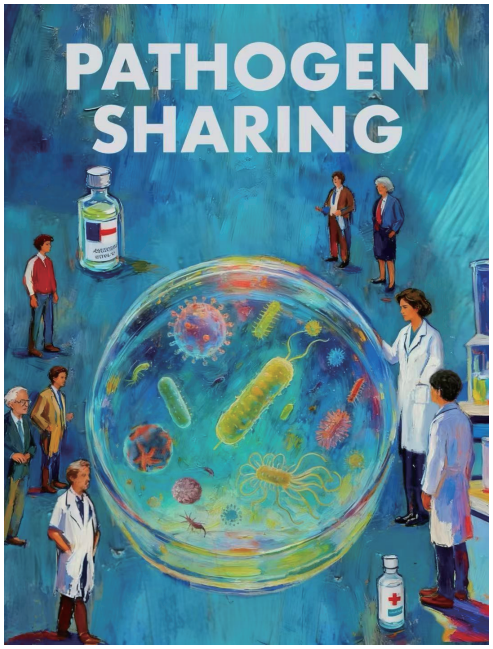

ISSN 2096-7071

China CDC Weekly

Editorial Board

Editorial Office

Cover Image: credited from the designer Jiaying Wang.

Commentary

Pathogen Access and Benefit-Sharing: Can the WHO Pandemic Agreement Bridge the Equity Divide?

Long Chen[1,2,#]

ABSTRACT

The adoption of the WHO Pandemic Agreement in May 2025 marks a pivotal shift toward institutionalizing global pandemic governance. Anchored in principles of equity, solidarity, and human rights, the agreement establishes a Pathogen Access and Benefit-Sharing (PABS) System, which aims to ensure equitable access to pandemic-related health products (PRHPs). However, operational ambiguities — particularly in defining pathogen scope, integrating traditional knowledge, enforcing manufacturer obligations, and coordinating with multilateral frameworks like the Convention on Biological Diversity and the Nagoya Protocol — pose significant implementation risks. Crucially, the agreement's effectiveness is intertwined with broader health system resilience. However, specific provisions for PABS integration within a strengthened health system architecture remain underdeveloped. Moreover, critical gaps persist regarding financing, compliance, One Health integration, digital governance, community engagement, and alignment with broader health systems. The success of the agreement hinges on resolving these gaps through subsequent protocols and sustained political commitment.

The coronavirus disease 2019 (COVID-19) pandemic has exposed some critical flaws in global health security, such as fragmented supply chains, vaccine nationalism, and systemic inequities in accessing diagnostics, therapeutics, and vaccines (*1*). Consequently, World Health Organization (WHO) member states initiated negotiations for a legally binding Pandemic Agreement in December 2021. After extensive deliberations, the agreement was adopted at the 78th World Health Assembly on May 20, 2025 (*2*). Its mandate is clear: transform ad hoc crisis responses into a cohesive, equity-driven framework for pandemic prevention, preparedness, and response. However, the success of this framework is intrinsically linked to underlying health system capacities and a broader preparedness ecosystem.

This commentary examines critical ambiguities within the Pathogen Access and Benefit-Sharing (PABS) mechanism established by the Pandemic Agreement. Key unresolved issues include defining pathogen scope (particularly those with zoonotic sources), enforcing manufacturer obligations for equitable product allocation, establishing transparent benefit-distribution criteria, and harmonizing the system with multilateral regimes such as the Convention on Biological Diversity (CBD) and the Nagoya Protocol. Furthermore, it explores foundational yet unaddressed issues, including specific compliance and financing models, the operationalization of One Health and digital equity principles, community-centric engagement frameworks, and mechanisms for resolving legal and ethical dilemmas arising from implementation. Future negotiations on the PABS operational protocol must urgently address these gaps to strengthen the mechanism and ensure effective implementation of the agreement.

Pathogen Access and Benefit-Sharing (PABS) System under the Pandemic Agreement

The Pandemic Agreement established the PABS system to advance global solidarity and address health equity challenges. Article 12 of the agreement mandates that parties rapidly share "materials and sequence information of pandemic-potential pathogens" and equitably distribute associated benefits based on the principles of justice and fairness. To operationalize this, the agreement implements a mechanism for allocating pandemic-related health products (PRHPs), contingent on a pandemic emergency declaration, as outlined by the following guidelines: 1) participating manufacturers must prioritize supplying 20% of the real-time production of

vaccines, therapeutics, and diagnostics targeting pandemic pathogens to the WHO under legally binding contracts; 2) this provision further specifies that no less than 10% of this allocation shall be donated, with the remainder provided at affordable prices commensurate with manufacturers' capacities. Critically, distribution must prioritize countries based on public health risk assessments, with explicit consideration for developing nations' needs.

However, the agreement establishes these obligations without specifying the requisite funding mechanisms to support LMIC implementation, nor does it define clear enforcement or incentive structures for manufacturer compliance, raising significant questions regarding its feasibility.

Core Implementation Challenges and Key Ambiguities in the Pathogen Access and Benefit-Sharing (PABS) Mechanism

Ambiguity in pathogen scope and the need for one health integration: Despite setting minimum standards for the PABS framework, Article 12 of the Pandemic Agreement fails to clearly define the scope of "materials and sequence information." Current negotiations have predominantly focused on human-derived pathogens and their genetic sequences. However, approximately 75% of emerging infectious diseases are zoonotic [e.g., severe acute respiratory syndrome (SARS) (*3*), Influenza A(H1N1) (*4*), Middle East respiratory syndrome (MERS) (*5*), Ebola virus disease (*6*), mpox (*7*), anthrax (*8*), and brucellosis (*9*)]. Consequently, it remains unclear whether the PABS system encompasses animal-sourced pathogens (e.g., wildlife and livestock) and broader microbiological agents (viruses, bacteria, fungi, and parasites). This narrow-scope risk undermines the agreement's preventive potential. Embedding an explicit One Health framework, mandating cross-sectoral data sharing, and joint risk assessment between the human, animal, and environmental health sectors is imperative to strengthen spillover prevention and comprehensive surveillance, which must explicitly delineate the covered pathogen types to ensure comprehensive surveillance.

Weak oversight and enforcement of manufacturer obligations: Under the obligations framework, Article 12 imposes two core requirements on manufacturers when a pandemic emergency is declared: donating 10% of their PRHP production to the WHO, and supplying an additional 10% at affordable prices. Notwithstanding these legally binding contractual commitments, one critical limitation is the agreement's lack of mechanisms to monitor compliance and define enforcement protocols. To ensure accountability, the operational protocol must establish an independent, multidisciplinary monitoring body with the authority to audit manufacturers' contributions and supply chains. This could be complemented by a tiered system of consequences for non-compliance, ranging from public reporting and financial penalties to exclusion from future publicly funded research and development partnerships, along with positive incentives such as preferential access to pathogen data or technology transfer pools for high-performing entities. Consequently, the current ambiguity risks inconsistent implementation, while simultaneously undermining accountability for equitable PRHP allocation.

Deficiencies in benefit-allocation equity and sustainable financing: Regarding benefit-distribution mechanisms, the PABS system exhibits critical flaws despite mandating manufacturers' contributions. Fundamentally, the "public health risk and need" principle lacks quantified parameters such as transmission coefficients and healthcare capacity, thereby enabling subjective interpretations. Furthermore, resource allocation faces ethical tensions between prioritizing high-transmission urban zones to curb the spread and vulnerable regions to prevent system collapse — a dilemma compounded by the absence of triage guidelines. Most critically, political capture risks emerge as high-income countries may leverage their bargaining power to divert resources. A fundamentally unresolved question is how to secure sustainable financing. The operational protocol should mandate the establishment of a dedicated, multi-source PABS implementation fund, potentially financed through assessed contributions from states; levies on manufacturers benefiting from PABS-shared materials; and multilateral donor funds, specifically earmarked to build regulatory, surveillance, and health system capacities in LMICs. The agreement also lacks sustainable financing mechanisms to support LMICs in implementing PABS obligations.

Challenges in multilateral framework complementarity and dispute resolution: Concerning institutional coherence, achieving complementarity between the PABS system and existing regimes presents several challenges. The primary focus of the negotiations has been the relationship with the CBD and the Nagoya Protocol, given the latter's requirements for prior informed consent and benefit-sharing of genetic resources. Defining the complementarity between these

systems is crucial to avoid legal uncertainties, particularly regarding pathogen sovereignty and access. Subsequently, jurisdictional overlap occurs in DSI governance; both the CBD's multilateral mechanism (Decision 16/2) and PABS claim authority over pathogen digital sequence information, potentially fragmenting the data infrastructure. Additionally, the agreement does not specify how equitable digital infrastructure and governance will be ensured, nor does it include clear dispute resolution mechanisms for conflicts between legal frameworks. Critically, the agreement lacks a dedicated mechanism for resolving conflicts that will inevitably arise between its provisions, the Nagoya Protocol, and the International Health Regulations. The establishment of an impartial technical arbitration panel or the referral of intractable legal disputes to an agreed-upon international judicial body should be considered to provide legal certainty and prevent diplomatic gridlock. Furthermore, the protocol should institutionalize a standing ethics advisory group to guide allocation decisions and resolve the ethical dilemmas inherent in prioritizing scarce resources.

The Path Forward: Addressing Critical Gaps Through Subsequent Negotiations

The Pandemic Agreement undoubtedly represents a pivotal moment for global health governance (*10*); nevertheless, its transformative promise remains contingent upon imperative actions that extend beyond its current text. First, finalizing the PABS operational annexes must specifically define the pathogen scope within an explicit One Health framework. Second, establishing robust and transparent monitoring and enforcement mechanisms for manufacturer obligations is non-negotiable. Third, creating a clear framework for complementarity with the Nagoya Protocol, coupled with a formal dispute-resolution mechanism, is essential. Moreover, the operational protocol must be considerably more ambitious, incorporating 1) legally binding and innovative sustainable financing mechanisms for LMICs; 2) mandates for equitable digital infrastructure and data governance; 3) operational frameworks for community engagement, trust building, and dynamic risk communication to counter misinformation and hesitancy; and 4) concrete obligations for upstream capacity building, including mandatory intellectual property sharing through multilateral pools and technology transfer initiatives to empower LMICs' production of PRHPs, thereby addressing inequities at their source. Critically, without these foundational and interconnected steps, the agreement risks perpetuating the health inequities that it seeks to resolve, thereby undermining its core mandate.

Conflicts of interest: No conflicts of interest.

Funding: Supported by the Sichuan Key Research Base of Philosophy and Social Sciences, Sichuan Center for Medical and Health Law Research (grant number: YF22-Y04).

doi: 10.46234/ccdcw2026.009

[#] Corresponding author: Long Chen, 0025131@zju.edu.cn.

[1] Guanghua Law School, Zhejiang University, Hangzhou City, Zhejiang Province, China; [2] Institute of Digital Jurisprudence, Zhejiang University, Hangzhou City, Zhejiang Province, China.

Submitted: June 28, 2025
Accepted: December 01, 2025
Issued: January 16, 2026

REFERENCES

1. Blinken AJ, Becerra X. Strengthening global health security and reforming the international health regulations: making the world safer from future pandemics. JAMA 2021;326(13):1255 – 6. https://doi.org/10.1001/jama.2021.15611.
2. WHO. Pandemic prevention, preparedness and response agreement. 2025. https://www.who.int/news-room/questions-and-answers/item/pandemic-prevention--preparedness-and-response-accord. [2025-06-27]
3. Dodd RY. Emerging infections, transfusion safety, and epidemiology. N Engl J Med 2003;349(13):1205 – 6. https://doi.org/10.1056/NEJMp038138.
4. Sooksawasdi Na Ayudhya S, Kuiken T. Reverse zoonosis of COVID-19: lessons from the 2009 influenza pandemic. Vet Pathol 2021;58(2):234 – 42. https://doi.org/10.1177/0300985820979843.
5. Han HJ, Yu H, Yu XJ. Evidence for zoonotic origins of middle East respiratory syndrome coronavirus. J Gen Virol 2016;97(2):274 – 80. https://doi.org/10.1099/jgv.0.000342.
6. Pourrut X, Kumulungui B, Wittmann T, Moussavou G, Délicat A, Yaba P, et al. The natural history of Ebola virus in Africa. Microbes Infect 2005;7(7-8):1005 – 14. https://doi.org/10.1016/j.micinf.2005.04.006.
7. Begeman L, van Riel D, Koopmans MPG, Kuiken T. The pathogenesis of zoonotic viral infections: lessons learned by studying reservoir hosts. Front Microbiol 2023;14:1151524. https://doi.org/10.3389/fmicb.2023.1151524.
8. Tahmo NB, Wirsiy FS, Nnamdi DB, Tongo M, Lawler JV, Broadhurst MJ, et al. An epidemiological synthesis of emerging and re-emerging zoonotic disease threats in Cameroon, 2000-2022: a systematic review. IJID Reg 2022;7:84 – 109. https://doi.org/10.1016/j.ijregi.2022.12.001.
9. Miller LN, Elmselati H, Fogarty AS, Farhat ME, Standley CJ, Abuabaid HM, et al. Using one health assessments to leverage endemic disease frameworks for emerging zoonotic disease threats in Libya. PLoS Glob Public Health 2023;3(7):e0002005. https://doi.org/10.1371/journal.pgph.0002005.
10. Schwalbe N. Pandemic treaty is a win for multilateralism and global health. BMJ 2025;389:r970. https://doi.org/10.1136/bmj.r970.

Vital Surveillances

Analysis of Rabies Epidemiological Characteristics and Failed Post-Exposure Prophylaxis Cases — Hunan Province, China, 2019–2024

Shengbao Chen[1]; Hao Yang[1]; Zhihong Deng[1]; Zhifei Zhan[1]; Zhihui Dai[1]; Fangling He[1]; Juan Wang[1]; Rongjiao Liu[1]; Ziqi Yang[1]; Kaiwei Luo[1,#]

ABSTRACT

Introduction: This study analyzed the epidemiological characteristics of rabies and the causes of post-exposure management failure in Hunan Province from 2019 to 2024, providing evidence for rabies prevention and control strategies in China.

Methods: Data on reported human rabies cases, exposures, and post-exposure prophylaxis (PEP) were analyzed using descriptive epidemiological methods.

Results: 240 rabies cases were reported in Hunan Province (2019–2024) with an average annual incidence rate of 0.0592 per 100,000 people. A significant decreasing trend was observed (χ^2_{trend}=32.72, P<0.05). Five factors showed statistically significant differences in their effects on the incubation period: site of exposure, wound management, vaccination after exposure, passive immunization preparations, and sources of animals causing exposure (all P<0.05). In the last six years, there was no increasing trend in the proportion of failed PEP as a percentage of all rabies cases in that year (χ^2_{trend}=1.809, P=0.86). The median incubation period was 16.0 (Interquartile Range, IQR 14.0–22.0) days for failed PEP cases with exposed areas, including to the head and/or face, compared to 31.0 (IQR 24.0–50.0) days for those without such exposure. The difference was statistically significant (U=20.50, P=0.025).

Conclusions: The current situation of rabies prevention and control in Hunan Province remains dire. Therefore, comprehensive measures should be implemented to help reduce the incidence of rabies. These include adopting standardized dog management practices, strengthening control measures in high-risk areas, and improving public awareness of PEP.

Rabies is an acute zoonotic disease caused by the rabies virus, clinically characterized by specific symptoms such as hydrophobia, aerophobia, agitation, and progressive paralysis. Once developed, the disease fatality rate is 100% (*1*). Rabies is highly endemic in Hunan Province, China. Although its incidence has decreased in recent years, the annual number of cases has always been among the highest in China, indicating a serious situation (*2*). Standardized and timely post-exposure wound management, vaccination, and the use of passive immunization preparations, if necessary, are key measures for preventing rabies. However, instances of post-exposure prophylactic failure (PEP) occasionally occur because of various influencing factors (*3*).

To understand the epidemiological characteristics of rabies and PEP failure cases in Hunan Province in recent years, information on rabies cases from 2019 to 2024 was organized and analyzed to provide a reference for future rabies prevention and control.

METHODS

Data Sources

Case data were derived from surveillance data reported to the China Information System for Disease Control and Prevention (CISDCP) and rabies case investigation records (2019–2024) in Hunan Province. When receiving reports of rabies cases from medical institutions, the local disease control center conducted epidemiological investigations on the cases and fills out the "Rabies Case Investigation Form," which includes the following: demographic characteristics; degree and location of wound exposure and disposal measures; use of rabies vaccine prophylaxis and passive immunization preparations; and characteristics of the animals causing exposure. Demographic data were obtained from the Hunan Statistical Compendium.

Definitions

Rabies diagnosis adhered to the *Diagnostic Criteria for Rabies* (WS 281-2008). The exposure severity was categorized according to the *Work Specification for Rabies Exposure Prophylaxis and Disposal* (2023 Edition) (*4*). A case of PEP failure was defined as a rabies death occurring despite receiving at least one of the following medical interventions after exposure: wound irrigation, rabies vaccination, or administration of passive immunizztion preparations (*5*–*6*).

Statistical Analysis

Data on rabies cases (2019–2024) in Hunan Province were collected and entered using EpiData software (version 3.1, Epidata Association, Denmark) and processed in Microsoft Excel 2021 (Microsoft Corporation, Redmond, WA, USA). SPSS Statistics (version 26.0, IBM, NY, USA) was then used to statistically describe and analyze the characteristics of rabies incidence and PEP failure cases. The overall incidence of rabies and the percentage of PEP failure cases were tested using the Cochran-Armitage trend test. The incubation period was described using median (Q1, Q3), and a comparative analysis was performed using the non-parametric Mann-Whitney U test. Statistical significance was defined as $P<0.05$.

RESULTS

Epidemiological Profile

Hunan Province reported 240 rabies cases between 2019 and 2024, including 128 clinically diagnosed and 112 laboratory-confirmed cases. The average annual incidence was 0.0592 per 100,000 individuals. A significant downward trend was observed over the study period ($\chi^2_{trend}=32.72$, $P<0.05$) (Figure 1).

Distribution of Disease

The highest number of cases was reported between July and October, with 102 cases accounting for 42.5% of the total. Cases were reported across all 14 prefectures, predominantly clustered in Shaoyang (77, 32.08%), Yongzhou (72, 30.00%), and Loudi (21, 8.75%). Males (n=170) outnumbered females (n=70) (male-to-female ratio: 2.43∶1). Their ages ranged from 2 to 90 years, with 65.42% (157/240) being concentrated in the 50–79 years age group. The majority comprised farmers (184, 76.67%), followed by students (26, 10.83%) and non-institutionalized children (13, 5.42%).

Characteristics of Animals Causing Exposure

Among the 240 cases, dogs accounted for 218 exposures (90.83%) and cats for 8 (3.33%), with the source unknown in 14 (5.83%) cases. Animal origins included household-owned (121/240, 50.42%), stray (63/240, 26.25%), and neighbor-owned (30/240, 12.50%) animals. Animal-initiated attacks, playing with animals, and animal self-defense injuries were the primary causes of injury, accounting for 35.42% of all injuries.

Exposure and Wound Management

Bites were the primary route of exposure (184/240, 76.67%), followed by scratches (20/240, 8.33%). The exposure severity was predominantly category III (156/240, 65.00%) or II (16/240, 6.67%). The exposure positions were categorized as such: hands (131/240, 54.58%); lower limbs distal to the knee

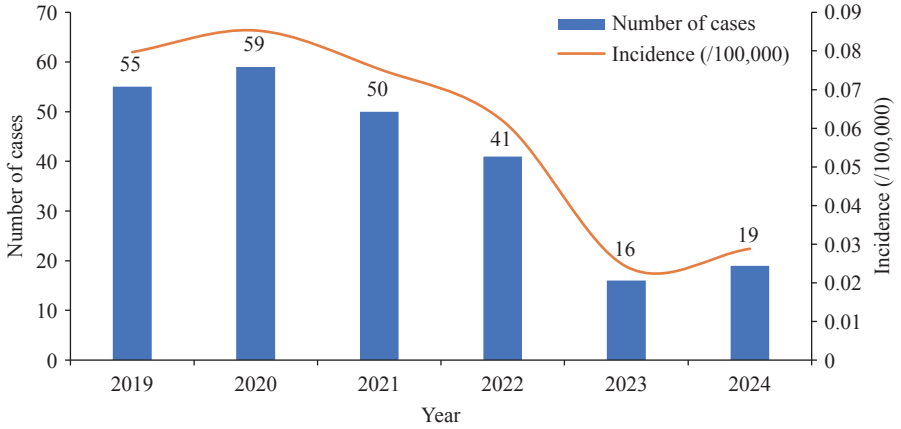

FIGURE 1. Trend of rabies incidence in Hunan Province, 2019–2024.

(35/240, 14.58%); and head/face/neck complex (15/240, 6.25%). Wound management status was as follows: no intervention (141/240, 58.75%); self-managed (77/240, 32.08%); and clinical management (22/240, 9.17%).

Post-exposure Prophylaxis

Among the 235 cases investigated for exposure immunization, none had a history of pre-exposure immunization. Eighteen (7.66%) patients were vaccinated with the human rabies virus vaccine after exposure. For category III exposures, 11/156 cases (7.05%) were administered passive immunization preparations.

Incubation Period Analysis

Among the 177 cases with confirmed incubation periods, the incubation period showed a right-skewed distribution (range: 1–1,774 days; median, 60 days). Non-parametric tests were used to analyze the influencing factors on the incubation period. The results showed that differences in the influences of five factors on the incubation period — exposure site, wound management, vaccination after exposure, passive immunization preparations, and the sources of the animal causing exposure — were statistically significant (P<0.05) (Table 1).

Analysis of PEP Failure Cases

Among the 240 rabies cases (2019–2024), 22 PEP

TABLE 1. The distribution of incubation period of rabies cases in Hunan Province, 2019–2024 (n=177).

Variables		Number of rabies cases (n)	Proportion (%)	Incubation period		Mean rank	Statistic (H/U)	P
				Median (day)	Q1–Q3			
Exposure type	Bite	154	87.01	65	30–133	90.52	4.169	0.244
	Scratch	14	7.91	60.5	32.5–150	88.75		
	Lick	4	2.26	23	†	37.88		
	Not specified	5	2.82	75	30–85	83.9		
Exposure category	Category Ⅲ	135	76.27	58	31–124.5	87.44	1.431	0.489
	Category Ⅱ	14	7.91	90	51.75–196.75	104.64		
	Not specified	28	15.82	65.5	31–99.75	88.7		
Exposure site	Hands	113	63.84	64	37–150	96.56	28.763	<0.001*
	Lower limbs below knee	25	14.12	42	24–71	64.22		
	Head and/or face	15	8.47	16	14–22.5	26.67		
	Lower limbs above knee	9	5.08	64	50–157	102.5		
	Trunk	3	1.69	60	†	99.33		
	Not specified	12	6.78	42	30–165	83.63		
Wound management	No intervention	88	49.72	73	39–150.25	100.24	25.507	<0.001*
	Self-managed	68	38.42	60	32–120	90.36		
	Clinical management	21	11.86	22	14–31	37.50		
Post-exposure vaccination	Yes	17	9.60	63.5	34–150	95.12	381.500	<0.001*
	No	160	90.40	16	14–24	31.44		
Post-exposure injection of passive immunization preparations	Yes	11	6.21	60	32–141.5	92.32	362.500	0.001*
	No	166	93.79	16	14–36	38.95		
Types of animals causing exposure	Dog	171	96.61	60	31–129.5	88.35	402.000	0.368
	Cat	6	3.39	77	50.75–133.25	107.50		
Sources of animals causing exposure	Household-owned	95	53.67	65	39–135	95.51	13.707	0.003*
	Neighbor-owned	24	13.56	55	23.25–152.5	83.67		
	Stray	51	28.81	39	30–67	72.54		
	Not specified	7	3.95	210	150–438	138.93		

* There are statistically significant differences between different groups of variables.
† The interquartile spacing could not be determined because the sample size was extremely small.

failures (9.17%) occurred, primarily in Shaoyang (nine cases) and Loudi (four cases). There was no increasing trend in the proportion of PEP failure in the last six years as a percentage of all rabies cases in that year (χ^2_{trend}=1.809, P=0.86).

Of the 22 cases of PEP failure, 15 were clinically diagnosed, seven were laboratory-confirmed, 18 were category III exposures, and four were of unknown exposure levels. There were 11 cases (50.00%) of head and/or face exposure, seven cases (31.82%) of hand exposure, and four cases (18.18%) of lower extremity exposure above and below the knee. Among all cases of PEP failure, 18 were vaccinated and 15 did not complete the full vaccination because they died after the onset of the disease. Additionally, three cases of category III exposure were involved in all aspects of PEP (wound management, vaccination, and administration of passive immunization preparations). The distribution of the PEP interventions by calendar year is shown in Table 2.

We also investigated the time from exposure to wound management in cases of PEP failure. Eighteen cases (81.82%) were treated on the day of exposure, while the remaining four cases were treated within 2–3 days after exposure. The shortest incubation period of PEP failure cases was two days, the longest was 209 days, and the incubation period was within three months in 16 cases (88.89%), with a median incubation period of 23.0 (14.0, 31.0) days. The median incubation period of failed PEP cases with exposed areas including head and/or face was 16.0 (14.0, 22.0) days, while it was 31.0 (24.0, 50.0) days for those without such exposure, with a statistically significant difference observed (U=20.50, P=0.025).

DISCUSSION

In this study, we retrospectively analyzed the trend of rabies incidence and the characteristics of cases with PEP failure from 2019–2024 in Hunan Province. Consequently, we found that the rabies epidemic in Hunan was in line with the development trend of rabies epidemics in China (*2*).

Notably, the temporal distribution of rabies in Hunan Province between 2019 and 2024 was consistent with other researchers' findings, with a higher number of cases occurring in summer and autumn (*7*). The regional distribution was dominated by traditional rabies-endemic cities such as Shaoyang, Yongzhou, and Loudi. Among these cases, most comprised farmers, with the age range mostly above 60 years. These characteristics are consistent with those reported by other scholars in China (*8*) and may be related to residents' limited knowledge of rabies prevention in rural areas and their reduced ability to avoid animal attacks.

The cases were dominated by bites, followed by scratches, which is consistent with domestic studies (*9*). Among these, category III exposures accounted for 65.00%, which was considerably higher than that reported for wounds treated at canine outpatient clinics in China (*10*). The exposure sites were mainly the hands and the lower limbs, which may be related to the defensive posture adopted when attacked by animals (*11*). In terms of wound management, over 90% of the patients did not visit medical institutions for treatment. Similarly, more than 90% of the patients were not vaccinated, and among those with category III exposure, the proportion of patients not receiving passive immunization preparations exceeded

TABLE 2. The distribution of PEP interventions among PEP failure cases in Hunan Province, 2019–2024.

Year	Total cases	PEP failure cases	Proportion of cases in the current year (%)	PEP interventions				
				Wound management only	Wound management + Not fully vaccinated	Wound management + Full vaccination	Wound management + Passive immunization preparations + Not fully vaccinated	Wound management + Passive immunization preparations + Full vaccination
2019	55	4	7.27	2	0	0	2	0
2020	59	5	8.47	1	0	0	4	0
2021	50	4	8.00	1	2	0	1	0
2022	41	5	12.20	0	4	0	0	1
2023	16	1	6.25	0	0	0	1	0
2024	19	3	15.79	0	1	0	0	2
Total	240	22	9.17	4	7	0	8	3

Abbreviation: PEP=post-exposure prophylaxis.

90%. These facts indicate that many people fail to fully recognize the danger of rabies and tend to take chances after exposure (*12*).

Among the factors influencing the incubation period, head and/or face exposure has a shorter incubation period than exposure at other parts of the body, mainly due to the neurophilic nature of the rabies virus and the abundance of peripheral nerve tissues in the head and face, allowing the virus to reach the central nervous system before vaccine-induced protective neutralizing antibodies are produced (*13*). Our study revealed that patients who sought medical treatment exhibited shorter incubation periods, which is consistent with previous research, likely because these cases were more severely exposed or had exposure to the head and/or face (*14*).

Currently, there is no universally accepted definition for rabies PEP failure. This study investigated the potential risks of PEP failure under different preventive interventions. Regardless of the reasons — such as inadequate understanding of PEP protocols, financial constraints, or personal negligence — patients who fail to receive all recommended preventive measures and subsequently develop rabies should be explicitly classified as PEP failure (*5–6*). Analysis of 22 PEP failure cases revealed that three cases with category III exposure received complete PEP in different levels of medical institutions. Nonetheless, their exposed areas were not entirely on the head or face. Thus, in the PEP process, it is necessary to increase the compliance of exposed individuals to participate in the entire process. Additionally, the risk of PEP failure in different situations must be considered (*15*).

This study has certain limitations. First, rabies patients often died during the investigation or cases were reported by family members, making it difficult to grasp the true and accurate exposure and disposal situation. This incomplete information may have affected the conclusions of this study. Second, while a preliminary analysis of factors influencing the incubation period was conducted, a more in-depth analysis is required. Third, some human rabies cases were clinically diagnosed because specimens were not collected immediately and no laboratory results were available.

In conclusion, the current situation of rabies prevention and control in Hunan Province remains a challenge. Comprehensive measures should be taken, such as adopting standardized dog management, strengthening control measures in high-risk areas, and improving public awareness of PEP, which may help reduce the incidence of rabies in Hunan.

Conflicts of interest: No conflicts of interest.

doi: 10.46234/ccdcw2026.010

[#] Corresponding author: Kaiwei Luo, cfk@hncdc.com.

[1] Center for Disease Control and Prevention of Hunan Province (Hunan Academy of Preventive Medicine), Changsha City, Hunan Province, China.

Submitted: July 25, 2025
Accepted: December 19, 2025
Issued: January 16, 2026

REFERENCES

1. Feng Y, Ma JH, Sun S, Chi LJ, Kou ZY, Tu CC. Epidemiology of animal rabies-China, 2010-2020. China CDC Wkly 2021;3(39):815 – 8. https://doi.org/10.46234/ccdcw2021.202.
2. Qin Y, Zhang Q, Lai SJ, Chen QL, Ren Q, Yin WW, et al. Analysis of epidemic characteristics of human rabies in China in 2007-2023. Chin J Exp Clin Virol 2024;38(4):373 – 7. https://doi.org/10.3760/cma.j.cn112866-20240403-00055.
3. Guzman FD, Iwamoto Y, Saito N, Salva EP, Dimaano EM, Nishizono A, et al. Clinical, epidemiological, and spatial features of human rabies cases in Metro Manila, the Philippines from 2006 to 2015. PLoS Negl Trop Dis 2022;16(7):e0010595. https://doi.org/10.1371/journal.pntd.0010595.
4. National Disease Control and Prevention Administration. Work specification for rabies exposure prophylaxis and disposal (2023 version). 2023. https://www.ndcpa.gov.cn/jbkzzx/c100012/common/content/content_1706568784078565376.html. (In Chinese). [2025-07-01].
5. Whitehouse ER, Mandra A, Bonwitt J, Beasley EA, Taliano J, Rao AK. Human rabies despite post-exposure prophylaxis: a systematic review of fatal breakthrough infections after zoonotic exposures. Lancet Infect Dis 2023;23(5):e167 – 74. https://doi.org/10.1016/S1473-3099(22)00641-7.
6. Wang SQ, Gao LD, Hu SX, Zeng G, Liu FQ, Guo SH. Epidemiological analysis of failed prevention and treatment cases after exposure to rabies. Contemp Med 2010;16(28):154-6. http://dx.doi.org/10.3969/j.issn.1009-4393.2010.28.124. (In Chinese).
7. Qin XA, Zhao HX, Shao ZJ. Study on the spatiotemporal distribution characteristics of rabies and the driving effects of meteorological factors in China from 2004 to 2019. J Air Force Med Univ 2024;45(5):531 – 6. https://doi.org/10.13276/j.issn.2097-1656.2024.05.010.
8. Zhu MT, Mu D, Chen QL, Chen N, Zhang YP, Yin WW, et al. Awareness towards rabies and exposure rate and treatment of dog-bite injuries among rural residents-Guangxi Zhuang Autonomous Region, China, 2021. China CDC Wkly 2021;3(53):1139 – 42. https://doi.org/10.46234/ccdcw2021.260.
9. Li TT, Jiao LX, Zhang LX, Luo JJ. Epidemiological characteristics of rabies and factors influencing its incubation period in Hubei Province, 2017-2021. Pract Prev Med 2023;30(9):1078 – 82. https://doi.org/10.3969/j.issn.1006-3110.2023.09.012.
10. Li GW, Tong H, Guo L, Wang WW, Jiang J. Analysis on epidemic characteristics and incidence trend of rabies exposed population in the city of Yichang from 2015 to 2019. J Med Pest Control 2021;37(1):19 – 22. https://doi.org/10.7629/yxdwfz202101005.
11. Gao Y, Ding XB, Li WH, Liu YY, Zhang CH, Yang XX. Current situation of animal injury among school children in Chongqing. J

Public Health Prev Med 2022;33(2):47 – 51. https://doi.org/10.3969/j.issn.1006-2483.2022.02.010.
12. Zhu ZH, Luo M, Zeng SQ, Zhu Q, Zhang M, Zhao JG, et al. Vaccination status of grade Ⅱ and Ⅲ rabies exposers in rabies post-exposure prophylaxis clinics and their influencing factors in Guangdong Province, 2019. South China J Prev Med 2025;51(1):118 – 22. https://doi.org/10.12183/j.scjpm.2025.0118.
13. Bykowski MR, Shakir S, Naran S, Smith DM, Goldstein JA, Grunwaldt L, et al. Pediatric dog bite prevention: are we barking up the wrong tree or just not barking loud enough. Pediatr Emerg Care 2019;35(9):618 – 23. https://doi.org/10.1097/PEC.0000000000001132.
14. Song KF, Wang SQ, Luo JJ, Huang JG, Hou QB, Wang L. Epidemiological characteristics of rabies and post-exposure immunization failure cases in Hubei Province in 2015-2021. J Public Health Prev Med 2023;34(4):35 – 8,127. https://doi.org/10.3969/j.issn.1006-2483.2023.04.008.
15. Zhang XM, Tian XY, Pang B, Wang ZQ, Zhai WJ, Jiang XL, et al. Epidemiological Characteristics of human rabies - Shandong Province, China, 2010-2020. China CDC Wkly 2022;4(35):793 – 7. https://doi.org/10.46234/ccdcw2022.055.

Methods and Applications

Validation of the Rapid Fluorescent Focus Inhibition Test for Rabies Virus Neutralizing Antibodies — China, 2025

Zixin Fang[1]; Xiaoyan Tao[1]; Shuqing Liu[1]; Qian Liu[1]; Minghui Zhang[1]; Nuo Yang[1]; Zeheng Hu[2]; Tom Jin[2]; Eric Tsao[2]; Pengcheng Yu[1,#]; Wuyang Zhu[1]

ABSTRACT

Introduction: The rapid fluorescent focus inhibition test (RFFIT) is a cell-based virus neutralization assay and the gold standard for quantifying rabies virus neutralizing antibodies (RVNA) in serums. It is used to assess the biological efficacy of rabies vaccines and evaluate protective immunity in both humans and animals. Despite its broad application, RFFIT requires thorough validation to ensure reliability.

Methods: RFFIT was validated in this study using the third World Health Organization international standard for anti-rabies immunoglobulin (WHO-3 SRIG) and negative human sera. The validation followed the guidelines outlined by the Food and Drug Administration Guidance for Industry and International Council for Harmonisation of Technical Requirements for Pharmaceuticals for Human Use (ICH)Q2 (R1) guidelines and included the assessment of intra-assay and intermediate precision, dilutability, linearity, range, accuracy, specificity, robustness, and stability.

Results: The RFFIT method demonstrated good precision, with intra-assay and intermediate-precision geometric coefficient of variation (GCV) <30%. Dilutability was confirmed, with 95% of positive samples showing geometric mean concentration (GMC) differences within ±30% compared to undiluted controls. The standard and detection values were described by y=1.0091x – 0.1128 (R^2=0.9948); 95.56% of the samples showed 70%–130% recovery. Specificity was verified using homologous and heterologous antigen competition and a matrix with no significant cross-reactivity. The assay was robust to variations in cells, reagents, and time, with titer differences within ±30%. Stability of samples and reagents under freeze–thaw and different short-term storage conditions was confirmed.

Conclusion: The assay was successfully validated for quantifying RVNA content in serum samples.

The rabies virus belongs to the Rhabdoviridae family and *Lyssavirus* genus and causes the fatal zoonotic disease, rabies (*1*). Once the symptoms of rabies appear, the fatality rate is 100%. Globally, an estimated 59,000 people die from rabies each year, with the majority of cases occurring in Asia and Africa (*2*). Effective prevention of rabies relies on timely vaccination, which is both a core component of post-exposure prophylaxis (PEP) and an important measure for pre-exposure immunization in high-risk populations (*3*).

Following rabies vaccination, a serum rabies virus neutralizing antibody titer of at least 0.5 IU/mL is considered indicative of an adequate immune response for effective protection (*4–5*). Serological testing is crucial for assessing the immunogenicity of rabies vaccines and for verifying protective antibody levels in vaccinated individuals. Of the existing testing methods, rapid fluorescent focus inhibition test (RFFIT) is considered the gold standard for the quantitative detection of rabies virus neutralizing antibodies (RVNA) (*6*).

RFFIT is a cell-based viral neutralization assay widely used to evaluate the biological efficacy of rabies vaccines and determine protective antibody levels in humans and animals. However, the complex analytical procedures of the assay may be affected by multiple factors, including cell line growth, reagent batch variations, and sample quality (*7–8*). A comprehensive validation of RFFIT was conducted in this study and confirmed RFFIT to be a reliable and standardized testing tool suitable for the serological surveillance and immunological assessment of rabies.

METHODS

Serum Samples

Fifty serum samples were prepared. 20 RVNA-positive serum samples (RVNA ≥0.5 IU/mL), 20 corresponding 1∶10 diluted RVNA-positive samples, and 10 RVNA-negative samples (Supplementary Table S1, available at https://weekly.chinacdc.cn/). Negative samples were obtained from pooled human serum. The RVNA-positive samples were prepared by mixing the third World Health Organization international standard for anti-rabies immunoglobulin (WHO-3 SRIG) (164 IU/mL) with pooled human serum. All samples were heat inactivated at 56 °C for 30 min prior to use.

In this study, the number of samples in the different serum groups aimed to efficiently use limited standard and serum matrices while covering all necessary concentration ranges. This approach also simulated the distribution of antibodies in real-world scenarios. Following vaccination, antibody levels in most individuals cluster within the low-to-moderate concentration range (close to the 0.5 IU/mL threshold). The validation results accurately reflected real-world testing scenarios by allocating more replicate samples to common concentrations, thereby enabling a more representative assessment of the reliability of the method.

Cells and Rabies Virus

The BSR cells are a clone of hamster kidney cells (BHK-21). BSR cells were maintained in Dulbecco's modified Eagle's medium (DMEM; Gibco, Cat. 11965092) supplemented with 10% fetal bovine serum (FBS; Gibco, Cat. 10091-148), 1% Penicillin–Streptomycin at 37 °C in a 5% CO_2 atmosphere. The challenge virus standard (CVS)-11 is a fixed strain that serves as an international standard challenge virus for rabies.

Heterologous Virus Antigens

Heterologous virus antigens were provided by Sinovac, China: Hepatitis A (38,355 U/mL, Batch No. 01-E2108-012); H1N1 flu (434 μg/mL, Batch No. A1-2205-037-SD); and EV71 (340 U/μg, Batch No. 08-E2111-006).

Pooled Human Sera

Pooled human serum was donated by volunteers at Synermore, all confirmed to be without a history of rabies virus exposure and with an RVNA titer of <0.5 IU/mL. A total of 13 individual serum samples were pooled and stored at −75±15 °C.

Matrix Sera

A 2% hemolytic matrix was prepared by mixing a hemolysis blood collection with an RVNA-negative whole blood sample. A lipemic matrix, a stock solution of 200 mg/mL triglycerides, was first prepared from glycerol trioleate (Aladdin, Catalog No. G105172-1g). The lipemic matrix, which contained 4.0 mg/mL triglycerides, was achieved by mixing the stock solution with the pooled human serum. The icteric matrix was formed by mixing 200 mg/L bilirubin with the pooled human serum (final concentration of bilirubin was 34.2 μmol/L; bilirubin was from MeilunBio, Dalian, China; Catalog No. MB1035-1).

Standard for Anti-Rabies Immunoglobulin

WHO-3 SRIG (Cat. No. 19/244, 164 IU) was diluted to 54.6667 IU/mL according to the manufacturer's instructions, and was used as a calibrator to calculate the RVNA titers (IU/mL) in the test serum samples.

RFFIT Protocol

The RFFIT procedure (*9*–*10*) was used to measure the level of RVNA against the CVS-11 strain of rabies virus in the serum samples. Heat-inactivated serum samples were serially diluted in a three-fold series and incubated with the CVS-11 strain in 96-well tissue culture plates at 37 °C for 60 min.

BSR cells were then added to the serum–virus mixture and incubated for an additional 24 h at 37 °C in a 5% CO_2 environment. The culture plates were fixed with acetone and stained with an anti-rabies N-FITC (fluorescein isothiocyanate) conjugate. Observation was conducted using a fluorescence microscope (IX2-ILL100, Tokyo, Japan, Olympus), and the percentage of infected cells was estimated by the reader; the percentage within two wells was recorded before and after 50% of the cells were infected. Finally, the Reed–Muench method (*11*) was applied to calculate the 50% end-point titer using the percentage of infected values.

RFFIT Validation

The validation plan was based on the Food and Drug Administration (FDA) Guidance for Industry

(*12*) and International Council for Harmonisation of Technical Requirements for Pharmaceuticals for Human Use (ICH) Q2 (R1) guidelines (*13*), considering the limitations and variability of cell-based virus neutralization assays. The FDA and ICH guidelines recommend a coefficient of variation (CV) of 15%–20% as the acceptance criterion for precision and accuracy in analytical method validation (*12*). However, the WHO notes that cell-based assays are expected to have a much higher CV (*14*). The RFFIT is a bioassay. Therefore, this RFFIT validation, a geometric coefficient of variation (GCV) of ≤30% was implemented. The validation parameters and acceptance criteria are listed in Table 1.

Precision and dilutability. Precision was evaluated at two levels: intra-assay precision (repeatability) and intermediate precision. Precision and dilutability were evaluated using the same set of 50 serum samples and analyzed in triplicate in six independent assay runs by two qualified analysts.

Accuracy, linearity, and range. The WHO-3 SRIG was serially diluted 2^3- to 2^{12}-fold to obtain concentrations from 20.5 to 0.0400 IU/mL. These dilutions were spiked into undiluted RVNA-negative serum samples to produce six concentrations: ULOQ 20.5 IU/mL, high quality control (HQC) 10.25 IU/mL, medium quality control (MQC) 2.5625 IU/mL, low quality control (LQC) 0.6406 IU/mL, LLOQ 0.0801 IU/mL, and LLD 0.0400 IU/mL. Each level was tested individually across six independent runs by two qualified analysts in triplicate for each run.

Specificity. Specificity was evaluated using antigen competition and matrix effect studies. For competition studies, 7 RVNA-positive samples (4 at 5.125 IU/mL and 3 at 2.5625 IU/mL) were pre-incubated separately with 5 serial 2-fold dilutions of homologous inactivated rabies virus (PV2061, Speeda, Chenda Bio, Liaoning, China), inactivated heterologous viruses (Hepatitis A virus, H1N1 influenza virus, and Enterovirus 71), and assay medium (baseline control).

For the matrix effect studies, 10 RVNA-positive samples (2 at 10.25 IU/mL, 4 at 5.125 IU/mL, 4 at 2.5625 IU/mL) were spiked in a 1:1 ratio with hemolytic, lipemic, and icteric matrices, and RVNA-negative serum (baseline).

Robustness. Robustness was assessed by varying the assay conditions for the RVNA titers. The impact of the BSR cells was evaluated by the percentage difference in the RVNA titer (5.125 IU/mL) from different BSR passages (P20, P30, P40, P60, P70, and P80). Additionally, BSR cells were inoculated and passaged every 2 or 3 days, and RFFIT tests were performed using 10 RVNA positive samples (4 of 5.125 IU/mL, 4 of 2.5625 IU/mL and 2 of 1.2813 IU/mL).

Further robustness testing was conducted using different batches and suppliers of the anti-rabies N-FITC conjugates and DMEM. The impact of reagent

TABLE 1. Validation parameters and acceptance criteria for the RFFIT for quantifying RVNA.

Validation parameter	Acceptance criterion	Remark
Intra-assay precision (repeatability)	GCV ≤30%	Criteria adjusted to cell-based assay performance
Intermediate precision	GCV ≤30%	Criteria adjusted to cell-based assay performance
Dilutability	≥80% samples show ≤30% GMC difference compared to undiluted control samples	
Determination of range (LLOQ, LLD, and ULOQ)	LLOQ: GCV ≤30%	Criteria adjusted to cell-based assay performance
Linearity	Linear regression slope must be 0.80–1.25 R^2 must be ≥0.95	
Accuracy	80% of the spiked SRIGs with results ≥LLOQ, with 70%–130% recovery of SRIG	Accuracy criteria should be met for the samples near the LLOQ level
Specificity-competition studies	(1) High-titer samples: Dose-dependent inhibition observed; ≥80% titer drop at highest concentration (2) Low-titer samples: Titer <LLOQ at highest concentration (3) Titer drop ≤30% *vs.* no-competition control	(1)(2) Applicable to competition with homologous antigens (3) Applicable to competition with heterologous antigens
Specificity - matrix effect	≥80% of matrix samples differed by ≤30%	Compared with normal serum
Robustness	RVNA titer differences within ±30% under varied conditions	
Stability	RVNA titer differences are within ±30%	

Abbreviation: RFFIT=rapid fluorescent focus inhibition test; RVNA=rabies virus neutralizing antibodie; GCV=geometric coefficient of variation; GMC=geometric mean concentration; LLOQ=lower limit of quantification; LLD=lower limit of detection; ULOQ=upper limit of quantification; WHO-3 SRIG=third World Health Organization international standard for anti-rabies immunoglobulin.

variation was assessed by comparing the RVNA titers (5.125 IU/mL) obtained from each batch/supplier. The assay was evaluated under various critical conditions.

Stability. The short-term stability of rabies virus, serum samples, and WHO-3 SRIG was assessed under various conditions. Serum samples (5.125 IU/mL) were assessed following 5 freeze–thaw cycles, and after 24 h, 1 w, and 4 w of storage at 4 ℃, and after 4 h at room temperature (20–25 ℃). The WHO-3 SRIG was assessed following 5 freeze–thaw cycles. The rabies virus stability was evaluated after 15 min at room temperature before use.

RESULTS

Precision and Dilutability

Samples were grouped by theoretical titer and the GCV% was calculated from the mean of triplicate replicates per run. All individual-precision GCV values were <30%, with most values from 5%–20% (Figure 1A, B). All ten negative samples tested negative in all runs.

Using 20 undiluted and 1∶10 diluted, paired RVNA positive samples, 95% (19/20) of the samples tested had an absolute value of the percentage difference ≤ 30% between the value for each 1∶10 diluted and undiluted serum sample. Linear regression of the GMCs for these pairs showed an R^2=0.9738 and a slope=0.9629, within acceptable limits indicating good dilution linearity (Figure 1C).

Accuracy, Linearity and Range

Of the tested concentrations of WHO-3 SRIG-spiked samples, 95.56% (86/90) of those with results ≥ LLOQ exhibited percentage recoveries within the acceptable range of 70%–130%. The GCV% of the

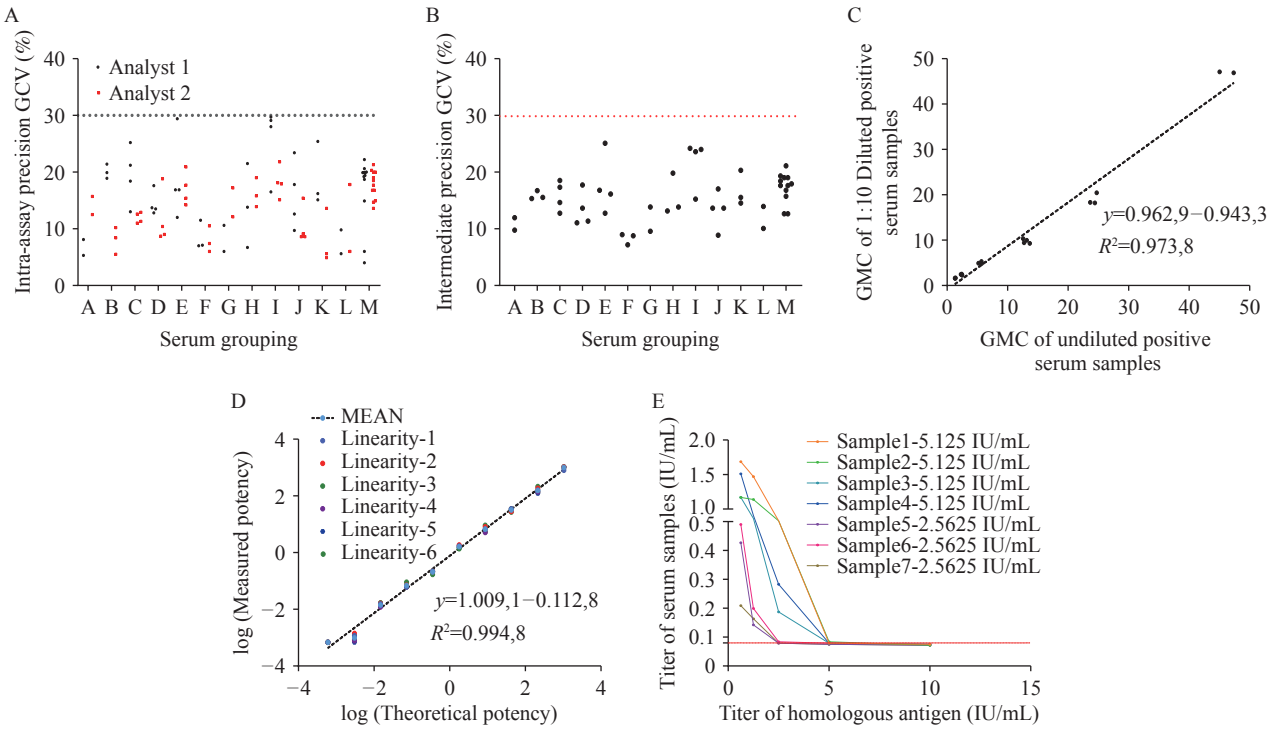

FIGURE 1. The results of RFFIT validation. (A) Summary of profile of the RFFIT intra-assay precision; (B) Summary of profile of the RFFIT intermediate precision; (C) Dilutability regression plot for the RFFIT using 20 paired RVNA positive samples; (D) Linearity of WHO-3 SRIG; (E) RFFIT specificity: dose-dependent inhibition with inactivated homologous competitor.

Note: In A and B, serum grouping: A, 44 IU/mL; B, 20.5 IU/mL; C, 10.25 IU/mL; D, 5.125 IU/mL; E, 2.5625 IU/mL; F, 1.2813 IU/mL; G, 4.4 IU/mL; H, 2.05 IU/mL; I, 1.025 IU/mL; J, 0.5125 IU/mL; K, 0.25625 IU/mL; L, 0.12813 IU/mL; M, RVNA negative samples. Each scatter point represents the repeated test geometric coefficient of variation values of the individual samples. In (D), MEAN represents the average of six results; In (E), red horizontal lines denote lower limit of quantification values.

Abbreviation: RFFIT=rapid fluorescent focus inhibition test; RVNA=rabies virus neutralizing antibodies; WHO-3 SRIG=third World Health Organization international standard for anti-rabies immunoglobulin.

LLOQ was <30%. Linear regression demonstrated strong correlation and acceptable linearity (slope=1.0091, R^2=0.9948), confirming that the accuracy and linearity acceptance criteria were met (Figure 1D).

Specificity

For homologous inactivated rabies virus antigen analysis, all samples showed dose-dependent inhibition (Figure 1E). At the highest competitor concentration, RVNA titers were reduced by ≥97% in high-titer samples, whereas low-titer samples fell below the LLOQ. In the heterologous antigen analysis, titer change in all samples was within assay variability (≤ 30%). Matrix effect evaluation showed that RVNA titers in hemolytic, icteric, and lipemic samples differed by ≤30% from normal serum. These results confirm the specificity of RFFIT.

Robustness

The RVNA titers (IU/mL) obtained from BSR cells at different passages exhibited differences within ±30%, with most variations being considerably smaller (e.g., −4.3% to 0.5%). Similarly, for cells tested on both day 2 and day 3 post-inoculation, the titer differences remained within an acceptable range, with the majority falling within ±25% (Table 2). Changes in experimental conditions resulted in percentage differences which were well within the ±30% range acceptable for cell-based assays (Table 3). These findings indicate that the assay was robust under various experimental conditions.

Stability

The titers measured for samples and standards under freeze–thaw and different storage temperature conditions were all within ±30% of the baseline value (Table 4).

TABLE 2. Impact of BSR cells and experimental conditions on robustness of RFFIT.

Condition		RVNA titer (IU/mL)	Difference (%)
BSR passages	Different days		
P20	2	5.1512	0.5
P30		5.1512	0.5
P40		4.9058	−4.3
P60		4.9272	−3.9
P70		4.9272	−3.9
P80		5.0578	−1.3
P81	2	5.7645	12.5
		5.7645	12.5
		5.5427	8.2
		6.0741	18.5
		2.1195	−17.3
		2.1195	−17.3
		2.2876	−10.7
		2.2876	−10.7
		1.0097	−21.2
		1.0097	−21.2
P81	3	6.0741	18.5
		5.8404	14.0
		5.8404	14.0
		6.4003	24.9
		2.4104	−5.9
		2.2334	−12.8
		2.2334	−12.8
		2.4104	−5.9
		1.0639	−17.0
		0.9921	−22.6

Note: The first section (rows 1–6) investigates the effect of cell passage number. The second section (rows 7–26) examines the impact of the cells on different days, which are specified for each group.
Abbreviation: RVNA=rabies virus neutralizing antibodies.

DISCUSSION

Various methods quantify RVNA. Commonly-used techniques include the mouse neutralization test (MNT), indirect immunofluorescence assay, RFFIT, fluorescent antibody virus neutralization test (FAVN), and enzyme-linked immunosorbent assay (ELISA). RFFIT is the most widely-used cell-based assay for detecting and quantifying rabies virus neutralizing antibodies in serum (*3*). Its results can be used for RVNA testing for pre- or post-exposure prophylaxis in humans or animals, as well as for the clinical diagnosis of rabies, detection of neutralizing activity of monoclonal antibodies against the rabies virus, determination of potency of immunoglobulin preparations, evaluation of the efficacy of new vaccines, development of new vaccination schedules, and evaluation and calibration of new serological testing methods (*10*). This validation supports the implementation of robust quality control measures and confirms the reliability of RFFIT for quantifying RVNA in serum.

Rabies antibody testing determines immunity levels conferred by pre- and post-exposure vaccinations.

TABLE 3. Impact of experimental conditions on robustness of RFFIT.

Incubation time	Critical reagents (Supplier/ Cat. No.)		RVNA titer (IU/mL)	Difference (%)
HI + SVN + PI + FITC	DMEM	FITC		
30 min + 50 min + 23 h + 50 min	Gibco/3023261	FUJIREBIO/311520	5.6156	9.6
30 min + 70 min + 25 h + 70 min	Gibco/3023261	FUJIREBIO/311520	5.5066	7.4
60 min + 60 min + 24 h + 60 min	Gibco/3023261	FUJIREBIO/311520	5.4707	6.7
30 min + 60 min + 24 h + 60 min	Sigma/RNBN1157	FUJIREBIO/311520	5.7269	11.7
30 min + 60 min + 24 h + 60 min	Gibco/3023261	FUJIREBIO/311624	5.7144	11.5
30 min + 60 min + 24 h + 60 min	Gibco/3023261	FUJIREBIO/311520	5.7144	11.5
30 min + 60 min + 24 h + 60 min	Gibco/3023261	Sigma/4206160	5.6156	9.6
30 min + 60 min + 24 h + 60 min	Gibco/3023261	FUJIREBIO/311520	5.0578	−1.3

Note: The section examines the impact of alterations in incubation time and critical reagents, which are specified for each group.
Abbreviation: DMEM=Dulbecco's modified Eagle's medium; HI=heat inactivation; SVN=serum virus neutralization; PI=post-infection; FITC=fluorescein isothiocyanate; RFFIT=rapid fluorescent focus inhibition test; RVNA=rabies virus neutralizing antibodies.

TABLE 4. Stability evaluation of the RFFIT.

Condition	RVNA titer (IU/mL)	Difference (%)
WHO-3 SRIG — 1 freeze–thaw cycle	39.2490	−28.2
WHO-3 SRIG — 2 freeze–thaw cycles	39.2490	−28.2
WHO-3 SRIG — 3 freeze–thaw cycles	39.2490	−28.2
WHO-3 SRIG — 4 freeze–thaw cycles	39.2490	−28.2
WHO-3 SRIG — 5 freeze–thaw cycles	44.1519	−19.2
Sample (5.125 IU/mL) — 1 freeze–thaw cycle	4.9058	−4.3
Sample (5.125 IU/mL) — 2 freeze–thaw cycles	4.9058	−4.3
Sample (5.125 IU/mL) — 3 freeze–thaw cycles	4.9058	−4.3
Sample (5.125 IU/mL) — 4 freeze–thaw cycles	4.9058	−4.3
Sample (5.125 IU/mL) — 5 freeze–thaw cycles	4.9058	−4.3
Sample (5.125 IU/mL): 4 ℃ 4 w	4.9058	−4.3
Sample (5.125 IU/mL): 4 ℃ 1 w	4.9058	−4.3
Sample (5.125 IU/mL): 4 ℃ 24 h	4.9058	−4.3
Sample (5.125 IU/mL): room temperature, 4 h	4.3610	−14.9
Rabies virus: room temperature, 15 min	4.9058	−4.3

Note: The baseline value of WHO-3 SRIG: 54.6667 IU/mL; room temperature: 20–25 ℃.
Abbreviation: RFFIT=rapid fluorescent focus inhibition test; RVNA=rabies virus neutralizing antibodies; WHO-3 SRIG=third World Health Organization international standard for anti-rabies immunoglobulin.

Although the intermediate precision met the acceptance criterion of ≤30% GCV, higher GCV values were generally observed in samples with low antibody titers near the critical threshold of 0.5 IU/mL. The WHO Rabies Expert Advisory Committee considers antibody levels ≥0.5 IU/mL in serum to indicate effective protection. If the antibody titer falls below 0.5 IU/mL, multiple booster doses should be administered until sufficient antibodies are produced. Therefore, accurate measurements around this cutoff are essential for determining seroconversion and adequate immune protection in clinical practice. The increased variability observed near this threshold can be attributed to the inherent limitations of serological assays at low analyte concentrations, including reduced signal-to-noise ratios and the impact of biological variability. Nevertheless, the RFFIT method still conformed to the pre-specified validation criterion of ≤30% GCV across all samples, underscoring its overall reliability.

This study has several limitations. First, validation was performed using serum spiked with WHO-3 SRIG rather than clinical samples from vaccinated individuals. Second, the sample size was limited (n=50)

and may not fully represent the diversity of immune responses across populations. Finally, precision was reduced near the critical threshold of 0.5 IU/mL.

In conclusion, this study demonstrated that the validated RFFIT method exhibited excellent analytical performance for quantifying RVNA in post-vaccination serum. The assay met all criteria for specificity, accuracy, precision, stability, linearity, and robustness, ensuring result integrity and reproducibility under varied conditions. These findings support the suitability of RFFIT for the reliable assessment of vaccine-induced immunity in both clinical and research settings (*15*). Its broader implementation for serological monitoring in rabies sero-surveillance and vaccine evaluation studies is recommended.

Conflicts of interest: The authors declare no conflicts of interest.

Ethical statements: This study did not involve human or animal subjects; therefore, no ethical statements were required.

doi: 10.46234/ccdcw2026.011

Corresponding author: Pengcheng Yu, yupc@ivdc.chinacdc.cn.

[1] NHC Key Laboratory of Medical Virology and Viral Diseases, National Institute for Viral Disease Control and Prevention, Chinese Center for Disease Control and Prevention & Chinese Academy of Preventive Medicine, Beijing, China; [2] Synermore Biologics (Suzhou) Co., Ltd., Suzhou City, Jiangsu Province, China.

Submitted: July 17, 2025
Accepted: November 24, 2025
Issued: January 16, 2026

REFERENCES

1. Fooks AR, Cliquet F, Finke S, Freuling C, Hemachudha T, Mani RS, et al. Rabies. Nat Rev Dis Primers 2017;3:17091. https://doi.org/10.1038/nrdp.2017.91.
2. Hampson K, Coudeville L, Lembo T, Sambo M, Kieffer A, Attlan M, et al. Estimating the global burden of endemic canine rabies. PLoS Negl Trop Dis 2015;9(4):e0003709. https://doi.org/10.1371/journal.pntd.0003709.
3. WHO Expert Consultation on rabies. World Health Organization technical report series. 2005;931:1-88.
4. Doornekamp L, Embregts CWE, Aron GI, Goeijenbier S, van de Vijver DAMC, van Gorp ECM, et al. Dried blood spot cards: a reliable sampling method to detect human antibodies against rabies virus. PLoS Negl Trop Dis 2020;14(10):e0008784. https://doi.org/10.1371/journal.pntd.0008784.
5. WHO. WHO expert consultation on rabies: WHO TRS N°1012: third report. Geneva: World Health Organization; 2018. https://www.who.int/publications/i/item/WHO-TRS-1012.
6. Ciconello FN, Katz ISS, Fernandes ER, Guedes F, Silva SR. A comparative review of serological assays for the detection of rabies virus-specific antibodies. Acta Trop 2022;226:106254. https://doi.org/10.1016/j.actatropica.2021.106254.
7. Proposed Revision of the Policy on Rabies Vaccines and Rabies Immunoglobulins. SAGE Working Group on Rabies Vaccines and Immunoglobulins/World Health Organization; 2017.
8. Timiryasova TM, Luo P, Zheng LY, Singer A, Zedar R, Garg S, et al. Rapid fluorescent focus inhibition test optimization and validation: Improved detection of neutralizing antibodies to rabies virus. J Immunol Methods 2019;474:112626. https://doi.org/10.1016/j.jim.2019.06.017.
9. Smith JS, Yager PA, Baer GM. A rapid reproducible test for determining rabies neutralizing antibody. Bull World Health Organ 1973;48(5):535-41. https://pubmed.ncbi.nlm.nih.gov/4544144/.
10. Yu PC, Lv XJ, Shen XX, Tang Q, Liang GD. Establishment and preliminary application of a rapid fluorescent focus inhibition test (RFFIT) for rabies virus. Virol Sin 2013;28(4):223 – 7. https://doi.org/10.1007/s12250-013-3321-x.
11. Reed LJ, Muench H. A simple method of estimating fifty per cent endpoints. Am J Epidemiol 1938;27(3):493 – 7. https://doi.org/10.1093/oxfordjournals.aje.a118408.
12. FDA. Guidance for Industry: bioanalytical method validation. Rockville, MD: Food and Drug Administration; 2001.
13. ICH. Q2(R1) Validation of analytical procedures: text and methodology. Geneva: ICH; 2005. https://www.fda.gov/media/152208/download.
14. WHO. WHO recommendations on rabies post-exposure treatment and the correct technique of intradermal immunization against rabies. Geneva: WHO; 1997. https://www.who.int/publications/i/item/who-wer7220.
15. Kostense S, Moore S, Companjen A, Bakker ABH, Marissen WE, von Eyben R, et al. Validation of the rapid fluorescent focus inhibition test for rabies virus-neutralizing antibodies in clinical samples. Antimicrob Agents Chemother 2012;56(7):3524 – 30. https://doi.org/10.1128/AAC.06179-11.

SUPPLEMENTARY MATERIAL

SUPPLEMENTARY TABLE S1. Detailed plan of positive and 1：10 human serum sample preparation.

No.	Volume of WHO-3 SRIG (164 IU/mL, μL)	Volume of pooled human serum (μL)	RVNA titer of positive serum sample (IU/mL)	RVNA titer of 1:10 diluted positive serum sample (IU/mL)
1	132.00	360.00	44	4.4
2	132.00	360.00	44	4.4
3	60.00	420.00	20.5	2.05
4	60.00	420.00	20.5	2.05
5	60.00	420.00	20.5	2.05
6	30.00	450.00	10.25	1.025
7	30.00	450.00	10.25	1.025
8	40.00	600.00	10.25	1.025
9	40.00	600.00	10.25	1.025
10	46.00	1,426.00	5.125	0.5125
11	27.00	837.00	5.125	0.5125
12	27.00	837.00	5.125	0.5125
13	27.00	837.00	5.125	0.5125
14	17.00	1,071.00	2.5625	0.25625
15	17.00	1,071.00	2.5625	0.25625
16	17.00	1,071.00	2.5625	0.25625
17	14.00	882.00	2.5625	0.25625
18	6.00	762.00	1.2813	0.12813
19	6.00	762.00	1.2813	0.12813
20	6.00	762.00	1.2813	0.12813

Abbreviation: No.=number; RFFIT=rapid fluorescent focus inhibition test; RVNA=rabies virus neutralizing antibodies; WHO-3 SRIG=third World Health Organization international standard for anti-rabies immunoglobulin.

Methods and Applications

Machine Learning Models for Predicting Latent Tuberculosis Infection Risk in Close Contacts of Patients with Pulmonary Tuberculosis — Henan Province, China, 2024

Dingyong Sun[1,&]; Xuan Wu[2,&]; Yanqiu Zhang[1]; Weidong Wang[1]; Mengya He[1]; Linqi Diao[1,#]

ABSTRACT

Introduction: We explored risk factors for latent tuberculosis infection (LTBI) and developed a risk prediction model using machine learning algorithms.

Methods: Patients with active pulmonary TB in months 3 to 6 of anti-TB treatment in Henan Province, China, July–September 2024 were selected as index cases. Close contacts identified through epidemiological investigation underwent tuberculin-purified protein derivative testing to determine LTBI status. Face-to-face questionnaires were conducted to collect epidemiological data. The dataset was divided into training and testing sets (6:4), using a fixed random seed. Five models — logistic regression (LR), decision tree (DT), random forest (RF), support vector machines (SVM), and multilayer perceptron (MLP) — were trained and evaluated using the mean squared error (MSE) and coefficient of determination. The test set was subjected to external validation. Receiver operating characteristic curve analysis, area under the curve (AUC), and F1-scores were used to quantify predictive performance.

Results: Among 795 close contacts, LTBI prevalence was 401 (50.5%). By MSE, models ranked: SVM (0.121), RF (0.165), DT (0.197), LR (0.229), and MLP (0.233). SVM identified five key predictors: contact type of index case, key population classification, residential area, frequency of participation in group activities, and etiological results. Internal validation showed strong performance (AUC=0.921, F1=0.858), whereas external validation showed moderate performance (AUC=0.752, F1=0.694).

Conclusion: The SVM model incorporating contact type of index case, key population classification, residential area, frequency of group activity participation, and etiological results demonstrated robust predictive value for LTBI risk. This model shows promise for the targeted screening and management of high-risk populations.

Latent tuberculosis infection (LTBI) refers to a chronic immune response to *Mycobacterium tuberculosis* antigens, without clinical or radiological evidence of active tuberculosis (ATB) (*1*). Prophylactic treatment of LTBI plays an increasingly pivotal role in TB control. It is estimated that 23% of the global population has LTBI (*2*), and the overall disease burden is relatively high in China. LTBI is a potential reservoir for ATB, with 5%–10% of the LTBI cases progressing to active disease. Therefore, LTBI treatment directly affects the global prevention of future TB infections. LTBI research largely relies on screening high-risk populations and developing targeted treatment strategies (*3*). Examining families and other close contacts of patients with ATB is warranted for the identification and management of LTBI (*4*–*6*).

Machine learning techniques such as support vector machines (SVM), random forest (RF), and artificial neural networks have been widely used in disease monitoring, diagnosis, and prognosis. These methods effectively detect novel patterns within existing datasets. In LTBI prediction, machine learning helps identify risk indicators that may remain undetected using conventional statistical approaches.

In this study, a survey and analysis of the close contacts of patients with TB in Henan Province were conducted. Five machine learning methods, namely, SVM, RF, decision tree (DT), logistic regression (LR), and multilayer perceptron (MLP), were used to predict LTBI. Their predictive accuracies were systematically compared to identify the optimal LTBI prediction framework. Furthermore, targeted interventions were proposed for high-risk populations identified using the best-performing model, enabling a proactive shift in TB prevention and control strategies.

METHODS

This study used a univariate logistic regression analysis for variable screening. Based on the 10 events per variable criterion, which requires a minimum sample size of 10–15 times the number of variables, 19 factors were analyzed. The estimated incidence of LTBI among close contacts of patients with pulmonary TB was approximately 30%. Therefore, the minimum number of required outcome events was 10×19=190. Consequently, the calculated minimum sample size was 190/0.3=634 participants. Allowing for 20% loss to follow-up, 760 close contacts were enrolled. To facilitate enrollment, the final target sample size was set to 800.

Index cases were identified through the Tuberculosis Management Information System (the China Disease Control and Prevention Information System) as patients with ATB in Henan Province receiving treatment for 3–6 months in 2024. LTBI was defined as individuals who shared the same residence for at least 7 days with an ATB patient during the period from 3 months before the patient's diagnosis to 14 days after diagnosis, and showed a strongly positive purified protein derivative (PPD) test result. Non-LTBI individuals were defined as those who were ruled out for both active and latent TB infection, with no more than one non-LTBI subject enrolled per patient as a study participant. A PPD test was performed according to the Chinese Guidelines for Preventive Treatment of Tuberculosis and the PPD results were recorded after 72 h. For PPD≥10 mm, ATB is ruled out based on the clinician's diagnosis, and the individual is determined to have latent TB infection. For PPD<10 mm, if active and latent tuberculosis infection are ruled out based on the clinician's diagnosis, the individual is classified as having a non-latent infection. LTBI cases were household contacts of patients with ATB (exposure≥7 days between 3 months pre- and 14 days post-diagnosis) with a strongly positive PPD test. Non-LTBI controls were excluded for both ATB and LTBI, with up to one control enrolled per patient. Close contacts of these index cases were recruited after written informed consent was obtained. After excluding individuals owing to employment-related migration, refusal to participate, or incomplete data during the field investigations, 795 close contacts were finally included. All contacts underwent tuberculin PPD testing and TB screening and completed structured questionnaires at designated TB care facilities. Questionnaire-derived variables and system-recorded clinical parameters of the index cases were analyzed as potential predictors of LTBI among close contacts.

The Delphi method was used to design the two structured questionnaires. First, the Index Case Questionnaire was completed by designated institutions based on medical records including demographic, diagnosis, and treatment information. The second questionnaire was completed by the investigator during in-person interviews with close contacts, supplemented by medical records retrieved from the case-reporting information system. The questionnaire included questions regarding sociodemographic characteristics, lifestyle habits, exposure history, and TB-related knowledge. If close contacts were unable to participate because of physical limitations, family members or guardians completed the questionnaire on their behalf. Provincial TB control institutions conducted city-level data verification, followed by double data entry using Epi Data 3.1 software (EpiData Association, Odense, Denmark). The finalized databases were securely transmitted to provincial authorities via encrypted emails.

A database was established using EpiData 3.1, with data collected in Microsoft Excel (Microsoft Office Home and Student 2019, Microsoft Corporation, Redmond, USA). Data analysis was conducted using SPSS Modeler (version 18.0; IBM Corp, Armonk, NY, USA) and SPSS 27.0. Qualitative data were analyzed using the chi-squared test followed by univariate logistic regression analysis. Machine learning models including SVM, RF, DT, MLP, and LR were developed to predict LTBI. The model performance was evaluated using the mean squared error (MSE) and coefficient of determination (R^2). A lower MAE and higher R^2 indicated superior predictive accuracy. The predictive values of these models were further assessed using receiver operating characteristic (ROC) curves and F1-scores, with external validation of the test set. The MSE, R^2, and area under the ROC curve (AUC) were calculated using SPSS 27.0, integrated with Python 3.12. A two-tailed test was applied, with statistical significance set at α =0.05.

RESULTS

Baseline Characteristics of Close Contacts

After excluding individuals with missing information owing to migrant work or refusal to

participate in the field investigation, 795 close contacts were included. LTBI accounted for 50.44% (n=401) of the close contacts. Significant differences (P<0.05) were observed between the LTBI and non-LTBI groups in terms of marital status, educational level, occupational type, residential area type, per capita living space, household registration type, annual household income, frequency of participation in group activities, type of contact with index cases, Bacille Calmette–Guérin (BCG) scar, weekly frequency of sleep deprivation, population classification of index cases, key population classification of index cases, and etiological results of index cases (Table 1).

Construction of Machine Learning Algorithm Models

Using LTBI status (binary outcome) as the dependent variable and those with statistical significance from the univariate analysis (Supplementary Table S1, available at https://weekly.chinacdc.cn/) as independent variables, the dataset was divided via a random seed method into training and test sets in a 6∶4 ratio. Risk prediction models were developed using the following algorithms: LR: Binomial logistic regression with forward stepwise selection. DT: C5.0 algorithm with default pruning parameters. RF: 100 decision trees (n_{tree}=100) with Gini impurity used for node splitting. SVM: Regularization parameter set to 10, and regression precision tolerance=0.1. MLP: Automatically determined number of hidden layer neurons, hyperbolic tangent activation function for hidden layers, and softmax activation for the output layer.

Efficiency Analysis of Machine Learning Models

The corresponding evaluation metrics were calculated using Python 3.12. MSE and R^2 were used to evaluate the prediction accuracy of the models generated using each classifier algorithm. MSE was used to measure the model's prediction error by calculating the square of the difference between the predicted and true values averaged across all samples. A smaller MSE suggests a better prediction performance. R^2 measures the variance in the dependent variable accounted for by the model, suggesting its goodness of fit. The R^2 values vary between 0 and 1, with values closer to 1 indicating a superior fit and better explanatory ability.

Models with a lower MSE and higher R^2 were deemed more precise. The prediction accuracies in descending order were as follows: SVM, RF, C5.0 (DT model), LR, and MLP. Classifier performance was further evaluated using sensitivity, specificity, and accuracy, with higher values indicating better performance. The SVM model outperformed the other algorithms in terms of these metrics (Table 2).

Machine Learning Model Verification

The AUC and F1-scores were used as the overall evaluation metrics to assess the model performance. The AUC is used to measure the overall discriminative performance of the classifier. The AUC value ranges from 0 to 1, with values closer to 1 suggesting better model performance. An AUC value of 0.5 indicates that the predictive ability of the model is equivalent to random guessing. The closer the ROC curve is to the upper left corner, the better the predictive value.

The F1-score is the reconciled average of precision (positive predictive value) and recall (sensitivity), offering a comprehensive measure of performance. In the case of an imbalanced dataset, the F1 score accounts for both false positives and false negatives. The score ranges from 0 to 1, with higher values indicating better comprehensive performance.

In this study, the SVM model achieved the highest performance in terms of both AUC and F1 scores, with values of 0.921 and 0.858, respectively, for internal validation, and 0.752 and 0.694, respectively, for external validation. Overall, the SVM model exhibited the best predictive performance (Supplementary Table S2, available at https://weekly.chinacdc.cn/).

As shown in Figure 1, the SVM model consistently yielded higher ROC curves in both the training and test datasets, indicating its superior classification performance compared with the other models. The overlapping ROC curves of the MLP and LR models suggest comparable performance. Notably, the RF and C5.0 DT models demonstrated divergent trends; in the training set, RF outperformed C5.0, whereas in the test set, C5.0 outperformed RF. This difference could be attributed to the small sample size of the test set.

The SVM-based LTBI risk-prediction model was developed using variables relevant to the univariate analysis. Repeated model iterations demonstrate stable variable importance rankings without considerable fluctuations. The training set showed 85.9% accuracy, and the test set showed 68.3% accuracy (Table 2).

The top five predictors of LTBI onset, ranked by variable importance, were: 1) type of contact with the index case (14.76%); 2) key population classification of

TABLE 1. Comparison of the baseline characteristics of close contacts.

Variant	LTBI (*n*=401)	Composition ratio (%)	non-LTBI (*n*=394)	Composition ratio (%)	*OR* (95% *CI*)	*P*	*VIF*
Sex						0.985	1.482
Male	157	39.2	154	39.1			
Female	244	60.8	240	60.9	0.997 (0.750, 1.326)		
Age groups (years)						0.065	1.487
15–18	12	3.0	11	2.8			
19–60	312	77.8	280	71.1	1.021 (0.444, 2.352)	0.960	
≥60	77	19.2	103	26.1	0.685 (0.287, 1.635)	0.394	
BMI (kg/m^2)						0.971	1.111
18.5–23.9	228	56.9	227	57.6			
<18.5	19	4.7	19	4.8	0.996 (0.514, 1.930)	0.990	
≥24	154	38.4	148	37.6	1.036 (0.774, 1.386)	0.812	
Marital status						**<0.001**	**1.679**
Unmarried	81	20.2	30	7.6			
Married	310	77.1	350	88.8	0.328 (0.210, 0.512)	<0.001	
Divorced/widowed	10	2.5	14	3.6	0.265 (0.106, 0.659)	0.004	
Education level						**<0.001**	**1.599**
Illiterate	36	9.0	41	10.4			
Primary/junior high school	185	52.5	232	58.9	0.908 (0.558, 1.479)	0.699	
High school and above	180	37.9	121	30.7	1.694 (1.024, 2.803)	0.040	
Careers						**<0.001**	**1.338**
Other	84	20.9	97	24.6			
Farmer	163	40.6	210	53.3	0.896 (0.627, 1.280)	0.547	
Student/teacher	77	19.2	24	6.1	3.705 (2.152, 6.379)	<0.001	
Healthcare/detainee	19	4.7	7	1.8	3.134 (1.256, 7.822)	0.014	
Homemaker/unemployed	58	14.5	56	14.2	1.196 (0.748, 1.912)	0.455	
Labor intensity						0.488	1.350
Light	261	65.1	248	62.9			
Moderate	128	31.9	138	35.0	0.881 (0.655, 1.186)	0.655	
Heavy	12	3.0	8	2.0	1.425 (0.573, 3.546)	0.573	
Residence type						**0.019**	**1.508**
Rural	206	51.4	235	59.6			
Urban	195	48.6	159	40.4	1.399 (1.057, 1.853)		
Per capita living area (m^2)						**<0.001**	**1.505**
≥20	320	79.8	349	88.6			
<20	81	20.2	45	11.4	1.963 (1.323, 2.913)		
Household registration type						**<0.001**	**1.298**
Local residence	319	79.6	349	88.6			
Migrant population	82	20.4	45	11.4	1.994 (1.344, 2.956)		
Annual household income (CNY)						**0.032**	**1.362**
<30,000	179	44.6	204	51.8			
30,000–50,000	143	35.7	107	27.2	1.523 (1.105, 2.100)	0.010	
>50,000	79	19.7	83	21.1	1.085 (0.751, 1.567)	0.665	

Continued

Variant	LTBI (*n*=401)	Composition ratio (%)	non-LTBI (*n*=394)	Composition ratio (%)	*OR* (95% *CI*)	*P*	*VIF*
Exposure to dust						0.489	1.355
No	382	95.3	371	94.2			
Yes	19	4.7	23	5.8	0.802 (0.430, 1.498)		
Daily ventilation frequency						**0.063**	**1.180**
0–1 time	118	29.4	106	26.9			
2–3 times	89	22.2	93	23.6	0.860 (0.581, 1.272)	0.449	
>3 times	190	47.4	180	45.7	0.948 (0.680, 1.322)	0.754	
None	4	1.0	15	3.8	0.240 (0.077, 0.744)	0.013	
Frequency of group activity participation per week						**<0.001**	**1.763**
Low	259	64.6	321	81.5			
Moderate	87	21.7	61	15.5	1.768 (1.226, 2.549)	0.002	
High	55	13.7	12	3.0	5.681 (2.979, 10.833)	<0.001	
Contact type						**<0.001**	**2.578**
Household	292	73.7	348	90.2			
Neighbor	13	3.3	10	2.6	1.549 (0.670, 3.585)	0.306	
Relative	16	4.0	15	3.9	1.271 (0.618, 2.615)	0.514	
Colleague/classmate	56	14.1	7	1.8	9.534 (4.280, 21.240)	<0.001	
Other	19	4.8	6	1.6	3.774 (1.488, 9.574)	0.005	
Health education received						0.996	1.247
Yes	225	56.1	221	56.1			
No	176	43.9	173	43.9	0.999 (0.755, 1.322)		
BCG scar						**<0.001**	**1.150**
Present	314	78.3	263	66.8			
Absent	87	21.7	131	33.2	0.556 (0.405, 0.764)		
Smoking status						0.312	1.106
Never	179	44.6	202	51.3			
Occasional	5	1.2	6	1.5	0.940 (0.282, 3.134)	0.920	
Frequent	75	18.7	56	14.2	1.511 (1.013, 2.256)	0.043	
Quit smoking	10	2.5	8	2.0	1.411 (0.545, 3.652)	0.478	
Passive smoking	132	32.9	122	31.0	1.221 (0.888, 1.678)	0.218	
Weekly frequency of sleep deprivation						**<0.001**	**1.291**
None	242	60.3	291	73.9			
1–2 times	56	14.0	48	12.2	1.403 (0.920, 2.138)	0.115	
3–5 times	53	13.2	35	8.9	1.821 (1.150, 2.884)	0.011	
>5 times	50	12.5	20	5.1	3.006 (1.742, 5.189)	<0.001	
Comorbidities						0.867	3.256
None	310	77.3	308	78.2			
One	75	18.7	67	17.0	1.112 (0.772, 1.603)	0.568	
Two	12	3.0	15	3.8	0.795 (0.366, 1.726)	0.562	
Three or more	4	1.0	4	1.0	0.994 (0.246, 4.008)	0.993	
Index case variables (source of infection status)							
Sex						0.942	1.103
Male	292	72.8	286	72.6			

Continued

Variant	LTBI (*n*=401)	Composition ratio (%)	non-LTBI (*n*=394)	Composition ratio (%)	*OR* (95% *CI*)	*P*	*VIF*
Female	109	27.2	108	27.4	0.989 (0.724, 1.351)	0.942	
Occupation						**<0.001**	**1.462**
Other	24	6.0	28	7.1			
Farmer	232	57.9	270	68.5	1.002 (0.565, 1.778)	0.993	
Student/teacher	88	21.9	36	9.1	2.852 (1.461, 5.568)	0.002	
Homemaker/unemployed	52	13.0	60	15.2	1.011 (0.523, 1.956)	0.974	
Healthcare worker	5	1.2	0	0.0	>100	0.999	
Key population classification						**<0.001**	**1.591**
No	261	65.1	304	77.2			
Diabetes	41	10.2	44	11.2	1.085 (0.688, 1.713)	0.725	
Silicosis	9	2.2	6	1.5	1.747 (0.614, 4.973)	0.296	
School or childcare staff	79	19.7	36	9.1	2.556 (1.667, 3.919)	<0.001	
Other	11	2.7	4	1.0	3.203 (1.008, 10.179)	0.048	
Diagnosis delay						0.063	1.178
No delay	155	38.7	178	45.2			
Delayed	246	61.3	216	54.8	1.308 (0.986, 1.735)		
Treatment category						0.179	1.119
New case	356	88.8	361	91.6			
Retreatment case	45	11.2	33	8.4	1.383 (0.862, 2.218)		
Etiological results						**0.027**	**1.126**
Negative/not tested	96	23.9	122	31.0			
Positive	305	76.1	272	69.0	1.425 (1.042, 1.950)		

Note: Bold number means statistical significance.
Abbreviation: *OR*=odds ratio; *CI*=confidence interval; BCG=Bacille Calmette–Guérin; CNY=Chinese Yuan; LTBI=latent tuberculosis infection; *VIF*=variance inflation factor.

the index case (12.36%); 3) residential area of close contacts (12.02%); 4) frequency of participation in group activities (11.25%); 5) etiological results of the index case (10.47%) (Table 3).

Result Interpretation

Through multi-factor logistic regression analysis, the factors output by the SVM were interpreted. The results showed that the index case was a classmates or colleagues, the index case being a key population with diabetes or silicosis, high frequency of group activity participation per week, the index case having positive etiological results, annual income exceeding 50,000 Chinese Yuan, sleep deprivation more than five times a week, and having scars were risk factors for the occurrence of latent TB infection. Living in an urban or migrant population was a protective factor (Supplementary Table S3, available at https://weekly.chinacdc.cn/).

DISCUSSION

Compared with conventional statistical methods, machine learning algorithms offer advantages such as higher accuracy, greater precision, and stronger adaptability. Moreover, they have been widely used for disease screening (*7*). In this study, data from patients with TB and their close contacts from different areas of Henan Province were analyzed to identify the optimal model for predicting LTBI. The training dataset was analyzed using SVM, RF, DT, MLP, and LR algorithms. The performance of the models were validated using a test dataset. The comparative evaluation indicated the following MSE rankings from lowest to highest: SVM (0.121), RF (0.165), C5.0 (0.197), LR (0.229), and MLP (0.233), confirming the superior predictive performance of SVM. The SVM model achieved an AUC of 0.921, F1-score of 0.858, sensitivity of 0.888, and specificity of 0.831. External validation yielded an AUC of 0.752, F1-score of

TABLE 2. Evaluation table of each classifier algorithm prediction model in the training set.

Model	Training set					Test set		
	MSE	R^2	Sensitivity	Specificity	Accuracy	Sensitivity	Specificity	Accuracy
LR	0.229	0.086	0.702	0.601	0.627	0.629	0.583	0.591
C5.0	0.197	0.215	0.734	0.730	0.732	0.644	0.689	0.665
RF	0.165	0.342	0.891	0.712	0.779	0.536	0.656	0.665
SVM	0.121	0.517	0.888	0.831	0.859	0.659	0.711	0.683
MLP	0.233	0.073	0.662	0.581	0.602	0.621	0.596	0.624

Abbreviation: MSE=mean squared error; LR=logistic regression; RF=random forest; SVM=support vector machines; MLP=multilayer perceptron.

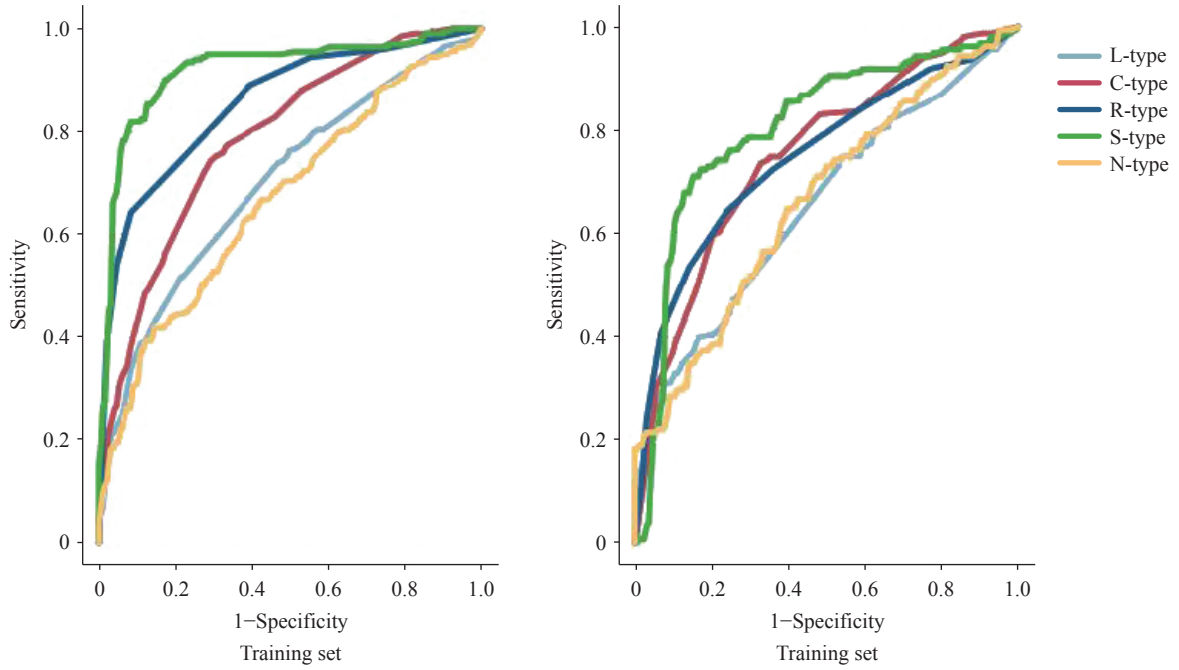

FIGURE 1. LTBI risk prediction model based on the SVM algorithm.
Abbreviation: SVM=Support vector machine; LTBI=Latent tuberculosis infection.

0.694, sensitivity of 0.659, and specificity of 0.711. These results demonstrate robust screening performance and strong alignment with accurate LTBI status.

SVM, a supervised binary classification model, excels in high-dimensional data analysis by isolating optimal decision boundaries, making it widely applicable in disease screening (*8*). Its advantages include reducing structural risk to enhance generalizability, optimizing both empirical risk and confidence intervals concurrently, and the capacity to efficiently learn from small datasets while maintaining statistical validity (*9*–*10*).

In this study, repeated iterations of the SVM model yielded stable rankings of variable importance. The top five predictors of LTBI were the type of contact with the index case (14.76%), key population classification of the index case (12.36%), residential area of close contact (12.02%), frequency of participation in group activities (11.25%), and etiological results of the index case (10.47%).

These findings suggest that close contacts who were coworkers or classmates of patients with pulmonary TB demonstrated a significantly higher risk of developing LTBI than contacts who lived in the same household. This observation aligns with the research conducted by Schepisi et al. (*11*) in school and congregate settings. Furthermore, this aligns with the increased risk of extrapulmonary transmission among nonhousehold contacts in urban African contexts, as reported by Kakaire et al. (*12*). This study also detected a dose-response relationship between the risk of LTBI and frequency of participation in group activities. Gathering in institutional settings (e.g.,

TABLE 3. Importance of input variables in LTBI risk prediction model based on SVM algorithm.

Variant	Importance of forecasting	Variant	Importance of forecasting	Variant	Importance of forecasting
Contact type	0.1476	Etiological results of index case	0.1047	Occupation of index case	0.0509
Key population classification of index case	0.1236	Household registration type	0.0891	BCG scar	0.0281
Residential area of close contact	0.1202	Annual household income	0.0712		
Frequency of group activity participation	0.1125	Weekly frequency of sleep deprivation	0.0568		

Abbreviation: SVM=support vector machines; LTBI=latent tuberculosis infection; BCG=Bacille Calmette–Guérin.

classrooms and meetings) prolongs exposure and intensifies interpersonal proximity. In overcrowded environments with poor ventilation, these conditions synergistically increase the risk of aerosol transmission by increasing the density of respiratory droplet exchange, extending the suspension time of *M. tuberculosis* in confined spaces, and reducing effective air exchange rates.

Additionally, close contact with bacteriologically positive pulmonary TB patients was associated with a greater risk of LTBI, consistent with the findings of Lei et al. (*13*). Patients with bacteriologically confirmed pulmonary TB have higher levels of *M. tuberculosis*, leading to stronger pathogenicity. Sputum and respiratory droplets are rich in bacilli, which increases the risk of infection. Finally, close contacts of index cases with severe diseases such as human immunodeficiency virus (HIV) infection are more likely to develop LTBI. HIV co-infection is the most critical risk factor for LTBI reactivation. HIV infection results in a reduction in the number of $CD4^+$T cells in both lymphoid tissues and peripheral blood. Elevated viral loads and rapid progression to acquired immunodeficiency syndrome (AIDS) are associated with an increased risk of LTBI (*14*). Finally, close contacts in rural areas were at a higher risk of developing LTBI. According to Gao et al., the estimated annual rate of TB in rural areas is 1.5%. The present study provides population-based evidence that older adults in rural China have a high prevalence of LTBI and relatively high risk of new infections (*15*–*16*).

In screening with limited data, interpretable models such as LR are often preferred because their advantages readily inform public health strategies. However, this study highlights the potential of machine learning for capturing complex data relationships, thereby laying the foundation for future multimodal integration. Thus, developing and validating advanced machine learning models remain essential for building precise automated screening systems in the long term.

Although machine learning offers advantages such as improved sensitivity, specificity, and diagnostic efficiency, it has some limitations. These shortcomings include the requirement for extensive datasets, poor interpretability of models, dependence on algorithms and technologies, and issues related to data privacy and security. Owing to variations in population distribution, prevalence rates, and other influencing factors that lead to a shift in data distribution, caution should be exercised when applying the model to other populations. As more data can help the model to generalize better, data from the target population will continue to be collected in the future, merged with source data, and used to train the model with a larger dataset. Individuals with LTBI may exert greater effort to recall and report risk factors related to TB. These biases can systematically distort the feature values and obscure the true distribution of certain predictors. Participants may underreport sensitive information, such as smoking or alcohol use, while potentially overreporting behaviors such as physical exercise. The specificity issues of the PPD test due to BCG vaccination and nontuberculous mycobacterial infection, as well as sensitivity issues due to immunosuppression, may have affected the estimation of the latent infection rates and risk factors in this study. Moreover, integrating machine learning models with biomarker-based diagnosis of *M. tuberculosis* infection may improve the application of prediction tools.

The findings in this report are subject to at least two limitations. First, the cross-sectional design can identify factors associated with LTBI, but cannot establish causality and may be susceptible to survivor bias. Second, despite controlling for multiple known risk factors, residual unmeasured confounding factors such as genetic factors and subtle environmental exposures may affect the model's feature importance and generalizability. Therefore, our findings should be regarded as an initial step toward more accurate identification of LTBI using machine learning. Future

studies should establish longitudinal cohorts with long-term follow-up for active TB outcomes to develop prognostic models that truly predict progression risk. Only through such efforts can artificial intelligence realize its full potential for optimizing TB prevention and enabling precision in public health.

In conclusion, this study suggests an SVM model constructed using machine learning algorithms focused on five predictors: types of close contacts, occupational types of the index case, residential locations of close contacts, frequency of participation in group activities, and etiological results of the index case. These factors showed strong predictive power for assessing the risk of LTBI. Through precise stratification, costly testing and treatment resources can be concentrated on those most in need, thereby avoiding wastage of low-risk populations. In large-scale community screenings, the rapid prioritization of a large number of individuals can be achieved, allowing limited human and material resources to maximize their effectiveness. Our next step will be to validate the model's performance across heterogeneous populations using multicenter data and explore hybrid models that integrate clinical variables with biomarkers.

Conflicts of interest: No conflicts of interest.

Funding: Supported by grants from Henan Provincial Science and Technology Development Program (Grant No. 242102311109).

doi: 10.46234/ccdcw2026.012

[#] Corresponding author: Linqi Diao, lqdiao@163.com.

[1] Department of Tuberculosis Prevention and Control Center, Henan Center for Disease Control and Prevention, Zhengzhou City, Henan Province, China; [2] Department of Epidemiology, School of Public Health, Zhengzhou University, Zhengzhou City, Henan Province, China.

[&] Joint first authors.

Submitted: August 28, 2025
Accepted: January 09, 2026
Issued: January 16, 2026

REFERENCES

1. Boom WH, Schaible UE, Achkar JM. The knowns and unknowns of latent *Mycobacterium tuberculosis* infection. J Clin Invest 2021;131(3): e136222. https://doi.org/10.1172/JCI136222.
2. Houben RMGJ, Dodd PJ. The global burden of latent tuberculosis infection: a re-estimation using mathematical modelling. PLoS Med 2016;13(10):e1002152. https://doi.org/10.1371/journal.pmed.1002152.
3. Ai JW, Ruan QL, Liu QH, Zhang WH. Updates on the risk factors for latent tuberculosis reactivation and their managements. Emerg Microbes Infect 2016;5(2):e10. https://doi.org/10.1038/emi.2016.10.
4. Velen K, Shingde RV, Ho J, Fox GJ. The effectiveness of contact investigation among contacts of tuberculosis patients: a systematic review and meta-analysis. Eur Respir J 2021;58(6):2100266. https://doi.org/10.1183/13993003.00266-2021.
5. Hook EB. Latent tuberculosis infection. N Engl J Med 2022;386(13): e33. https://doi.org/10.1056/NEJMc2200195.
6. Zhang CY, Liu YS, Yao YX, Gong DH, Lei RR, Xia YY, et al. Tuberculosis infection among close contacts of patients with pulmonary tuberculosis in China: a population-based, multicentered study. Clin Microbiol Infect 2024;30(9):1176 – 82. https://doi.org/10.1016/j.cmi.2024.06.003.
7. Li LS, Yang L, Zhuang L, Ye ZY, Zhao WG, Gong WP. From immunology to artificial intelligence: revolutionizing latent tuberculosis infection diagnosis with machine learning. Mil Med Res 2023;10(1):58. https://doi.org/10.1186/s40779-023-00490-8.
8. Sebro R, De la Garza-Ramos C. Opportunistic screening for osteoporosis and osteopenia from CT scans of the abdomen and pelvis using machine learning. Eur Radiol 2023;33(3):1812 – 23. https://doi.org/10.1007/s00330-022-09136-0.
9. Youssef Ali Amer A. Global-local least-squares support vector machine (GLocal-LS-SVM). PLoS One 2023;18(4):e0285131. https://doi.org/10.1371/journal.pone.0285131.
10. Wang HJ, Shao YH, Zhou SL, Zhang C, Xiu N. Support vector machine classifier via $L_{0/1}$ soft-margin loss. IEEE Trans Pattern Anal Mach Intell 2022;44(10):7253 – 65. https://doi.org/10.1109/TPAMI.2021.3092177.
11. Schepisi MS, Motta I, Dore S, Costa C, Sotgiu G, Girardi E. Tuberculosis transmission among children and adolescents in schools and other congregate settings: a systematic review. New Microbiol 2019;41(4):282-90. https://europepmc.org/article/MED/30252926.
12. Kakaire R, Kiwanuka N, Zalwango S, Sekandi JN, Quach THT, Castellanos ME, et al. Excess risk of tuberculosis infection among extra-household contacts of tuberculosis cases in an African city. Clin Infect Dis 2021;73(9):e3438 – 45. https://doi.org/10.1093/cid/ciaa1556.
13. Lei RR, Long HX, Luo CH, Yi BJ, Zhu XL, Wang QY, et al. Latent tuberculosis infection among close contacts of positive etiology pulmonary tuberculosis in Chongqing. Chin J Infect Control 2024;23(3):265 – 70. https://doi.org/10.12138/j.issn.1671-9638.20244977.
14. Sharan R, Bucşan AN, Ganatra S, Paiardini M, Mohan M, Mehra S, et al. Chronic immune activation in TB/HIV Co-infection. Trends Microbiol 2020;28(8):619 – 32. https://doi.org/10.1016/j.tim.2020.03.015.
15. Cui XJ, Gao L, Cao B. Management of latent tuberculosis infection in China: exploring solutions suitable for high-burden countries. Int J Infect Dis 2020;92S:S37-40. http://dx.doi.org/10.1016/j.ijid.2020.02.034.
16. Gao L, Li XW, Liu JM, Wang XH, Lu W, Bai LQ, et al. Incidence of active tuberculosis in individuals with latent tuberculosis infection in rural China: follow-up results of a population-based, multicentre, prospective cohort study. Lancet Infect Dis 2017;17(10):1053 – 61. https://doi.org/10.1016/S1473-3099(17)30402-4.

SUPPLEMENTARY MATERIAL

SUPPLEMENTARY TABLE S1. Variable assignment table.

Variant	Description of the assignment
Whether LTBI	Yes=1, No=0
Marital status	Unmarried=1, Married=2, Divorced/widowed=3
Educational level	Illiterate=1, Primary /Junior high school=2, High school and above=3
Occupation	Other=1, Farmer=2, Student/Teacher=3, Healthcare/Detainee=4, Homemaker/Unemployed=5
Residence type of close contact	Rural=1, Urban=2
Per capita living area	≥20 m^2=1, <20 m^2=2
Household registration type	Local residence=1, Migrant population=2
Annual household income	<30,000=1, 30,000–50,000=2, >50,000=3
Frequency of group activity participation	Low=1, Moderate=2, High=3
Contact type	Family member=1, Neighbor=2, Relative=3, Colleague/student=4, Other=5
BCG scar	Yes=1, No=2
Weekly frequency of sleep deprivation	None=1, 1–2 times=2, 3–5 times=3, >5 times=4
Occupation of index case	Other=1, Farmers=2, Students/teachers=3, Domestic workers=4, Medical workers=5
Key population classification of index case	Not a priority group=1, Diabetic=2, Silicosis=3, School or childcare staff=4, Other=5
Etiological results of index case	Negative/not detected=1, Positive=2

Abbreviation: LTBI=latent tuberculosis infection; BCG=Bacille Calmette–Guérin.

SUPPLEMENTARY TABLE S2. Evaluation table of the prediction model of each classifier algorithm in the test set.

Model	Training set		Test set	
	AUC	F1 score	AUC	F1 score
LR	0.688	0.583	0.653	0.547
C5.0	0.786	0.742	0.733	0.675
RF	0.862	0.723	0.691	0.570
SVM	0.921	0.858	0.752	0.694
MLP	0.667	0.559	0.662	0.578

Abbreviation: AUC=area under the curve; LR=logistic regression; RF=random forest; SVM=support vector machines; MLP=multilayer perceptron.

SUPPLEMENTARY TABLE S3. Multivariate analysis.

Variant	β	s_x	Wald χ^2	*OR* (95% *CI*)	*P*
Contact type			13.890		0.008
Household*					
Neighbor	0.616	0.440	1.960	1.851 (0.782, 4.383)	0.162
Relative	0.085	0.384	0.049	1.088 (0.513, 2.309)	0.826
Colleague/classmate	1.644	0.489	11.292	5.177 (1.984, 13.509)	0.001
Other	0.913	0.700	1.701	2.492 (0.632, 9.823)	0.192
Key population classification			4.872		0.301
No*					
Diabetes	0.758	0.385	3.887	2.135 (1.004, 4.537)	0.049
Silicosis	0.907	0.447	4.107	2.476 (1.030, 5.952)	0.043
School or childcare staff	0.606	0.425	2.028	1.833 (0.796, 4.220)	0.154
Other	22.029	17967	0.000	0.000	0.999
Residential area of close contact					
Rural*					
Urban	−0.176	0.175	1.011	0.838 (0.595, 1.182)	0.315
Frequency of group activity participation per week			7.544		0.023
Low*					
Moderate	0.349	0.201	3.007	1.417 (0.956, 2.102)	0.083
High	1.092	0.474	5.300	2.980 (1.176, 7.548)	0.021
Etiological results of index case					
Negative/not tested*					
Positive	0.484	0.176	7.563	1.623 (1.149, 2.291)	0.006
Household registration type					
Local residence*					
Migrant population	−0.321	0.242	1.756	0.725 (0.451, 1.166)	0.185
Annual household income (CNY)			6.232		0.044
<30,000*					
30,000–50,000	0.253	0.225	1.258	1.287 (0.828, 2.002)	0.362
>50,000	0.555	0.232	5.714	1.742 (1.105, 2.747)	0.017
Weekly frequency of sleep deprivation			12.235		0.007
None*					
1–2 times	−0.040	0.242	0.028	0.961 (0.598, 1.543)	0.868
3–5 times	−1.138	0.363	9.843	1.249 (0.745, 2.093)	0.339
>5 times	−0.843	0.377	5.005	2.710 (1.526, 4.813)	0.001
Occupation			4.370		0.358
Other*					
Farmer	−22.334	17964	0.000	0.000	0.999
Student/teacher	−21.591	17964	0.000	0.000	0.999
Homemaker/unemployed	−3.330	22270	0.000	0.036	1.000
Healthcare worker	−21.864	17964	0.000	0.000	0.999
BCG scar					
Present*					
Absent	0.361	0.175	4.246	1.434 (1.018, 2.021)	0.039

Abbreviation: BCG=Bacille Calmette–Guérin; *OR*=odds ratio; CNY=Chinese Yuan; *CI*=confidence interval.
* When performing multivariate analysis for each group of variable categories, the first variable is used as the reference.

Youth Editorial Board

Indexed by Science Citation Index Expanded (SCIE), Social Sciences Citation Index (SSCI), PubMed Central (PMC), Scopus, Chinese Scientific and Technical Papers and Citations, and Chinese Science Citation Database (CSCD)

The inauguration of *China CDC Weekly* is in part supported by Project for Enhancing International Impact of China STM Journals Category D (PIIJ2-D-04-(2018)) of China Association for Science and Technology (CAST).

CHINA CDC WEEKLY

CCDC weekly

Vol. 8 No. 3 Jan. 16, 2026

中国疾病预防控制中心周报(英文)

Responsible Authority
National Disease Control and Prevention Administration

Sponsor
Chinese Center for Disease Control and Prevention

Editor-in-Chief
Jianwei Wang

Editing and Publishing
China CDC Weekly Editorial Office
No.155 Changbai Road, Changping District, Beijing, China
Tel: 86-10-63150501, 63150701
Email: weekly@chinacdc.cn

Printing: Beijing Kexin Printing Co., Ltd

Complimentary Access

CSSN
ISSN 2096-7071 (Print)
ISSN 2097-3101 (Online)
CN 10-1629/R1